ASSESSMENT OF LAKE TUMBA WATER QUALITY EMPLOYING REMOTE SENSING, LANDSAT 8 IMAGES

A DISSERTATION REPORT

Submitted in partial fulfilment of the

requirements for the award of the degree

of

MASTER OF TECHNOLOGY

in

HYDROLOGY

by

LUSE TSHIDIBI

DEPARTMENT OF HYDROLOGY

INDIAN INSTITUTE OF TECHNOLOGY ROORKEE

ROORKEE – 247 667 (INDIA)

June 2019

CANDIDATE'S DECLARATION

I hereby certify that the work which is being presented in this report entitled, "**ASSESSMENT OF LAKE TUMBA WATER QUALITY EMPLOYING REMOTE SENSING, LANDSAT 8 OLI IMAGES"**, in partial fulfilment of the requirements for award of the degree of **Master of Technology in Hydrology** submitted to the Department of Hydrology, Indian Institute of Technology Roorkee, Roorkee is an authentic record of my own work carried out under the guidance of **Dr Himanshu Joshi, Professor, Department of Hydrology, IIT Roorkee** during the period from July 2018 to June 2019.

The matter embodied in this dissertation has not been submitted by me for the award of any other degree.

Date: ……June, 2019

LUSE TSHIDIBI**,**

Enrolment number 17537014

CERTIFICATE

This is to certify that the above statement made by the candidate is correct to the best of my knowledge.

Dr Himanshu Joshi,

Professor,

Department of Hydrology,

Indian Institute of Technology Roorkee,

Roorkee – 247 667 (Uttarakhand), India

ACKNOWLEDGEMENTS

First of all, I would like to thank God Almighty for his blessings to enable me to complete my studies and empower me to complete my research work. Without his blessings and grace, this achievement would not be possible.

With a very special sense of gratefulness, I would like to express my thanks to my supervisor **Dr Himanshu Joshi, Professor at Department of Hydrology** for his dedicated assistance, willingness to give his time, comments, and constructive suggestions throughout this work.

I would like to express my heartfelt thanks to Dr M. K. Jain, Head, Department of Hydrology, Dr M. Perumal, Dr D. S. Arya, Dr N.K Goel, Dr B. K. Yadav, Dr Sumit Sen, and Dr Jaya Khanna, Faculty Members, **Department of Hydrology, Indian Institute of Technology, Roorkee** for their excellent guidance, valuable teaching, assistance and encouragement during the entire course of my study at IIT Roorkee.

Further gratefulness goes to **ITEC Programme of Government of India**, which sponsored my study in Master of Technology (Hydrology) program of IIT Roorkee.

I also recognize and appreciate the lifelong influences of my elder brother Crispin TSHIBINKUFUA, siblings and friends whose personal sacrifices showed me the way of achieving my goal.

I express my sincere thanks to Summit Kumar PhD scholar, department of civil engineering of IIT Roorkee for his support and assistance during this study.

Also, I would like to thank all my fellow colleagues and friends for their constant help and encouragement during the course of the study. The help received from the staff members Department of Hydrology and other staff members of IIT Roorkee is thankfully acknowledged.

Dated: ….. June, 2019 **LUSE TSHIDIBI**

ABSTRACT

Lake Tumba has been chosen in this particular study because of the far-reaching role it plays in the Congo's basin. It is a water body harboring many kinds of fish and other aquatic organisms, and constitutes an important water supply source for the surrounding villages. The quality of lake Tumba is till now not too much impaired apparently due to less human activities taking place in the catchment. This study attempts to map and estimate lake Tumba water quality in terms of variables like TSS, TP and *Chl-a* concentration, employing remote sensing techniques (Landsat 8 OLI data). Concentration of various water quality variables (viz. Temperature, pH, DO, Turbidity, TSS, TP and *Chl-a*) was obtained at 18 points spatially distributed through the lake monitored physically in the months of September and October 2018.

This study employies remote sensing techniques (Landsat 8 OLI data) combined with a limited number of monitored field water quality parameter samples. Regression models were implemented using band ratios mean reflectance values to predict measured water quality variables. Turbidity did not give good result for both September and October conditions. Only three parameters (TSS, TP and ***Chl-a***) were taken into consideration in this particular study. The September image was also too much impacted by clouds. Therefore, only the clear portion of the lake was extracted for regression analysis purpose. The clear part of the lake contained only 9 sampling points out of 18, which were considered in the analysis for September. TSS concentrations were ranging from 1.2-2.8mgl/l for September monitoring.

High levels of TSS were recorded near inflow village Ikoko. TP and *Chl-a* concentrations were ranging from 1.6-3.5 mug/l; and 0.018-0.038 mug/l respectively and were found near lake surface5, inflow lokongoli, village Ikoko, and lake surface1, lake surface2, village lokongoli and village nkoso respectively. Concentration of TSS and *Chl-a* could successfully be estimated through remote sensing for September. However, similar estimation could not show a good result for October. This could be due to the impact of clouds held up in the ninth band of October image. Only TP estimation was successful for October using entire spatial information of the lake Tumba water quality. The temporal variation in the September and October water quality data did not emerge to be significant.

The Land Use Land Cover classified maps obtained from ESA allowed a study of the change detection in different components in the catchment area. The findings of this research laid

a foundation for successfully employing remote sensing techniques for estimation and mapping of lake Tumba water quality parameters in future field monitoring studies for facilitating the overall management of this lake.

TABLE OF CONTENTS

LIST OF TABLES

LIST OF FIGURES

LIST OF ABBREVIATIONS

APHA	The American Public Health Association
BNDVI	Blue normalized difference vegetation index
Chl-a	*Chlorophyll-a*
DNs	Digital Numbers
DO	Dissolved oxygen
DRC	Democratic Republic of the Congo
EPA	The Environmental Protection Agency
ESA	European Space Agency
FAO	Food and Agriculture Organization
GNDVI	Green Normalized difference vegetation index
GPS	Global Positioning System
IBDO	Improved Based Dark Object
IR	Infrared
LDCM	Landsat Continuity Mission
LULC	Land Use Land Cover
Max	Maximum
Mg/l	milligram per liter
Min	minimum
MLC	Maximum Likehood Classifier
μgl^{-1}	microgram per liter
MW	Microwave
NDVI	Normalized Difference Vegetation Index
NPS	Nonpoint Source
Oct	October
OLI	Operational Land Imager
pH	Potential of Hydrogen
Sept	September
Std	Standard deviation
SWIR	Shortwave Infrared

Tb	Turbidity
TIRS	Thermal infrared sensor
TP	Total phosphorus
TSS	Total Suspended Solids
UTM	The Universal Transverse Mercator
USGS	United States Geological Survey
WHO	The World Health Organization

CHAPTER ONE

INTRODUCTION

1.1 General

Fresh water bodies, the world's most important natural resources are in these last decades undergoing threats from a large number of agents, including adverse effects from agriculture, Land Use and Cover change related consequences, and also from other enormous man-made activities (Romshoo and Rashid 2012; Torbick et al., 2013; Mushtaq and Pandey, 2014). Most of people in the world are living closer to water resources and carry out activities responsible for nutrient enrichment and algal in water bodies (Torbick et al., 2013). High concentration of nutrients and sediments in lakes and reservoirs is the result of artificial sources like excess use of fertilizers in agriculture, poorly managed urban waste system along with climate change consequences (Kondratyev et al., 1998). Upward rate of manmade activities and global perturbation of natural systems have led to acute seasonal water shortage (Mushtaq and Pandey, 2014). Stress on water bodies will always grow up in the near future if any precaution is not taken into consideration, and many academic works have proved deterioration in water status conditions as one of important threats to human beings (Torbick et al., 2013).

Water quality assessment and monitoring play a far-reaching role and is very necessary task for each country to furnish water quality information to the public institutions and researchers in view of combating water quality problem. (Seker et al., 203; Chen et al., 2007). Water quality is generally described by its aesthetic (appearance and smell), biological, physical, chemical properties and is related to environmental Land Use and Land Cover behavior (Kostas et al., 2012). An adequate water quality assessment depends on a good field monitoring of water characteristics (Chapman, 1996). The use of monitoring in water quality assessment constitutes an important phase to describe water condition, to help determining trends and to provide useful information allowing establishment of a cause-effect relationship (Chapman, 1996).

Monitoring of water quality by routine methods relies on water sample collection and field/lab analyses, which may reasonably provide exact results; but the process is costly, tedious, skill and time demanding, and cannot give synchronous water quality data for large areas. (Brivio et al., 2001; Khattab MFO and Merkel BJ, 2013). This is particularly true for large water bodies

like lake Tumba, which is among the largest freshwater lakes in Africa. Unlike in situ measurements, remote sensing techniques have nowadays started to play a major role in assessment of water body status for large areas and provide identification and quantification of water quality variables and critical pollution problems for the impeccable management of surface water resources (Ritchie et al., 2003).

Using remote sensing techniques, surface water can entirely be monitored and assessed regularly and at a low cost. Relationships between water reflectance and monitored water quality variables are established using remote sensing technologies. Landsat images have been employed to predict and map water quality variables concentration in surface water. (Ritchie et al., 1990, Dekker and Peters, 1993; Wang et al., 2006).

Regression models are commonly applied to clearly show the correlation between monitored water quality variables and band reflectance values.

1.2 Objectives

The specific objectives in this study aim to:

- Employ the Landsat 8 satellite imageries for remote estimation of water quality variables in the lake Tumba, D.R. Congo.
- Evaluate the changes in the lake catchment over the past decades.

CHAPTER TWO

LITERATURE REVIEW

2.1 Water quality and its assessment

2.1.1 Water quality

The quality of water is an essential aspect of prime importance as life of human-beings depends on it. Water pollution may be defined as deterioration of the normal state, mainly when its physical, biological and chemical characteristics are impaired. Water may be considered as polluted when affected by man-made pollutant agents. Polluted water becomes dangerous for drinking purpose and aquatic life, especially for fish species. Water pollutants may originate from chemical compounds, or from infectious agents. Water pollution can be best considered in the perspective of possible pollutant cycles throughout the environment (Kumar De, 2018).

Some possible effects of polluted water are:

- disagreeable odour and colour.
- The proliferation of undesirable aquatic plants in water body.
- Death of large number of fish and other aquatic organisms.
- Oil and grease floating on water surfaces.

More than 700,000 of world's people does not have access to pure drinking water. More than one million of people lose their lives each year due to water-borne diseases and 27,000 children below five years die every week from water-borne diseases. In India, 1000 children die of diarrheal diseases every day. Many African and Asian countries are suffering and struggling due to water pollution issues (Kumar De, 2018). Sources of pollution can be classified into two main categories based on their origin as described in the following sections.

2.1.2 Point source

Point source pollution refers to each defined, constrained and independent conduit, including but not limited to any pipeline, duct, drain, tubing, canal, cylinder from which pollutant agents are or may be loaded into water. Leakage from tanks and mine tailings are also considered

as point source pollution, but storm water drained from agricultural fields and acid rains or irrigation with its return flows are not at all considered as point source pollution (EPA, 1994)

2.1.3 Nonpoint source

Nonpoint source pollution originates from many undiscernible sources. Rainfall or snowmelt running off on and in the ground are the main causes of NPS. As the rainfall water is running off, it collects all the artificial pollutant agents, ultimately discharges them into surface waters and even our drinking groundwater aquifers. These pollutants not only consist of all chemical products used in agriculture (insecticides, herbicides and fertilizers), but also all dangerous products originating from urban production of energy and runoff; precipitates from incorrectly controlled building places, from natural ecosystems (forest), and eroding streambanks. Acid drainage from deserted mines salt from irrigation practices, nutrients and bacteria from animal waste, breeding waste, sediments from atmosphere and hydro modification are also considered as nonpoint source pollution (EPA, 1994)

2.2 Water quality parameters relevant for remote sensing-aided assessment

2.2.1 Turbidity

Turbidity measures the extent to which light is scattered from a water body due to the suspended matter in water column, dissolved matter such as silt, clay, finite organic matter, plankton, other microscopic organisms, organic acids and decaying materials (Bilgehan Nas et al., 2010). Excluding not those suspended matters, fluorescent dissolved organic matter, colored dissolved organic matter and other dyes can also contribute to water turbidity (Anderson, 2005). Turbidity affects the physical look of water, making it to be hazy, dusky, opaque or gloomy. Thus, increase in turbidity conditions may facilitate waterborne disease. Inorganic constituents have no notable health effects (Koltas et al., 2012). Water clarity and appearance are also affected by turbidity. The estimation of total suspended matter in water quality assessment is an indicator of turbidity. Water turbidity always depends on the amount of the particles that are suspended in the main column of the water body (Perlman, H. 2014). The more suspended matter that is present, the less light penetration will be in the water body. Turbidity is a relative measure of water clarity, but not a direct measure of total suspended solids although both are related. The changes in

suspended matter concentration (without providing an accurate measurement of solids) can be indicated by measuring turbidity (EPA, 2012**).** The color produced from plant decomposition (dissolved substances) found in wetlands and other water bodies in high concentration affects the appearance of water, water tending to appear brown or red. Turbidity measurement takes into account these dissolved substances although they are too small in size and are not counted in suspended solids concentration. (Anderson, 2005).

Figure 2.1. Turbidity by TSS and vegetation decomposition

(Source: EPA, 2012)

2.2.2 Phosphorus

Phosphorus exists in water bodies in both dissolved and particulate forms. It is a determining factor for all living organisms. Phosphorus is an important element that governs lake's primary production and constitutes the limiting nutrient for algal growth. Increase in phosphorus concentrations, either naturally or artificially is the main cause of excessive nutrients in a water body (Chapman, 1996). Organic matter decomposition and weathering of P-bearing rocks are mainly the natural sources of phosphorus. Elevated levels of phosphorus in surface water are due to household wastes, especially waste waters that contain detergent, but also manufacturing discharges and chemical products run-off. Bacteria can mobilize and release phosphorus to water column when associated with mineral and organic constituents in water bodies (Chapman, 1996). Phosphorus is commonly incorporated in water quality monitoring programs as it is a contributing factor of biological cycle in water bodies. Increase in phosphate concentration can signify the

presence of water impairment and is largely the main cause the trophic status deterioration. Knowledge of the levels of phosphates is required particularly for drinking water supply in view of interpreting algae proliferation levels, and this is very important for lake management (Chapman, 1996). Phosphorus concentrations in laboratory are often estimated as total phosphorus, orthophosphates total or inorganic phosphate (combination of all phosphates and phosphorus).

2.2.3 *Chlorophyll-a*

Chlorophyll is commonly used as an indicator of water quality. It is a pigment found in all plants helping in photosynthesis process (Akbar T.A et al., 2009). Eutrophication refers to the presence of excess minerals and nutrients into a water body originating from natural and artificial sources, and their consequences on water resources (National Academy of Sciences, 1969). High concentrations of nutrients and minerals cause algal bloom and limit the sunlight to penetrate water column. Algae bloom entails depletion of oxygen required for aquatic life that leads to fish and other aquatic organisms' death. Estimation of algae biomass concentration that is present in a water column can be provided by *chlorophyll-a* measure (Hambrook et al., 2007). If *chlorophyll* levels in water body are known, phytoplankton biomass and chlorophyll-a can easily be estimated (EPA, 1989; Raschke, 1993). High concentrations of nutrients (main cause high *chlorophyll* levels in water body) originating from artificial sources like septic tanks discharge, badly managed wastewater systems, or fertilizer runoff can cause algal blooms that entails depletion of dissolved oxygen levels required for aquatic life, the primary cause of fish death. Estimation of *chlorophyll-a* concentrations can indicate the water quality state, trophic status and organic pollution levels; it is also an important parameter in managing water quality (Scherz J.P, 1972) and monitoring water pollution (Johson, R.W et al., 1980).

Figure 2.2. Eutrophication and algae bloom

(Source: EPA, 2012)

2.2.4 Total Suspended Solids

All substances whose size exceeds 2 microns (μ) present in a water body are known as total suspended solids. Every particle whose size is less than 2 microns (μ) is considered dissolved solid. TSS are essentially made of dead substances (inorganic), though algae and bacteria can also have contribution to TSS concentration in water body. Everything that floats or drifts on surface waters, from algal, precipitate, silt and sand to plankton are also considered as total solids (EPA, 2012). Organic particles originating from decaying can also be part of total suspended solids concentration. Micro organic particles detach and infiltrate water body as TSS through decaying process of algae plants and animals (Murphy, 2007). Suspended chemical products are considered as suspended solids (WHO, 2011).

Total suspended solids are determinant factor in evaluating physical look of water (EPA, 2014). Water clarity and suspended solids concentration are related. Some particles can decant into precipitate for couple of days at the bottom of a water body (EPA, 2014). Gravel and sand, heavier particles, when entering an area of low or no water flow, often settle out, improving water clarity. Increase in silt can smother fish eggs and benthic organisms (EPA, 2012). Other particles which do not settle out are called colloidal. They can also be called bedded sediments or bed load (EPA, 2012). They vary from fine (silt and clay) to larger (sand and gravel), based on the water flow rate. They can sometimes move downstream without being incorporated in TSS measure. The strong

flow makes them to move along the bottom of a water body. This process is called bed load transport (Wood et al., 2014).

Figure 2.3. TSS loading by erosion

(Source: EPA, 2012)

2.3 Remote sensing and water reflectance

2.3.1 Remote sensing

Remote sensing is the science of acquiring data about the earth objects or areas from far, without being in contact with them, generally from high flying aircraft or satellites. Remote sensing is divided into two types: Active sensors and Passive sensors. Active sensors produce their own source of light or illumination (artificial light) that is measured by the sensor as they reflect off the target; passive sensors systems just detect sun light (natural reflectance off the target). Passive remote sensing is effective if the involved satellite platforms maintain sun-synchronous orbits.

2.3.2 Water reflectance

Every substance in natural system and environment may be a subject of absorption, transmission, scattering, emission, and reflection of sunlight (electromagnetic spectrum portions). The quantity of sunlight that an object may release depends on wavelength or a specific frequency. Objects yielding different spectral properties do not have same spectral curves, thus making possible the distinction between the materials. To determine water status conditions, remote sensing techniques rely on electromagnetic radiation detection by sensors. Thus, surface waters

can be monitored based on the electromagnetic radiation detection because water scattering characteristics depend on the substances' type and concentration found in water (Shubha, 2000). Visible (VIS), Infrared (IR) and Microwave (MW) are the most important main spectral bands for assessing water bodies. (Richards, 1986; Schultz, 1988).

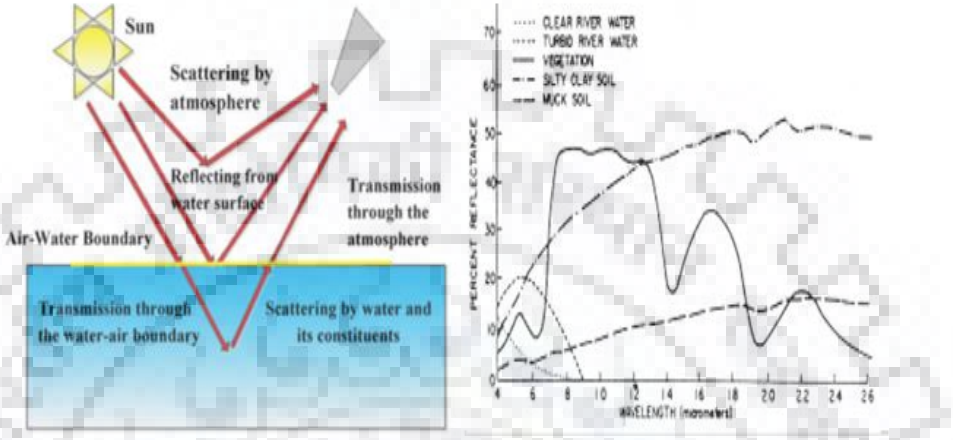

Figure 2.4. Water reflectance and spectral curve

(Source: Richards,1996)

2.3.3 Landsat 8

The Landsat Continuity Mission's (LDCM), Landsat 8 started operating in 2013, on 11th of February and has two sensors: OLI (Operational Land Imager) and TIRS (Thermal Infrared Sensor). It images the whole earth each 16 days in an 8-day offset from Landsat-7. The OLI instrument images the earth in the 9 spectral bands that cover the VIS, NIR and SWIR portion of the electromagnetic spectrum. Band 1 and band 9 dealing with aerosol studies (band 1) and clouds detection (band 9) have been added. All the 9 bands of OLI sensor in which the earth is imaged are acquired at the same resolution, means 30 meters except band 1 that is acquired at spatial resolution of 15 meters. The two long wavelength bands 10 and 11, are the thermal infrared bands in which TIRS sensor collects data. OLI data register 100-meter spatial resolution of TIRS for generating geometrically and radiometrically calibrated 16-bit level 1 data products, duly terrain-corrected. The thermal infrared bands (10, 11) are important because they provide more accuracy about temperatures generated by earth surface. (http://pubs.er.usgs.gov/publication/fs20133060). To characterize land cover state and conditions, OLI and TIRS offer ameliorated signal-to-noise radiometric performance quantized over 12-bit dynamic range (USGS, 2013).

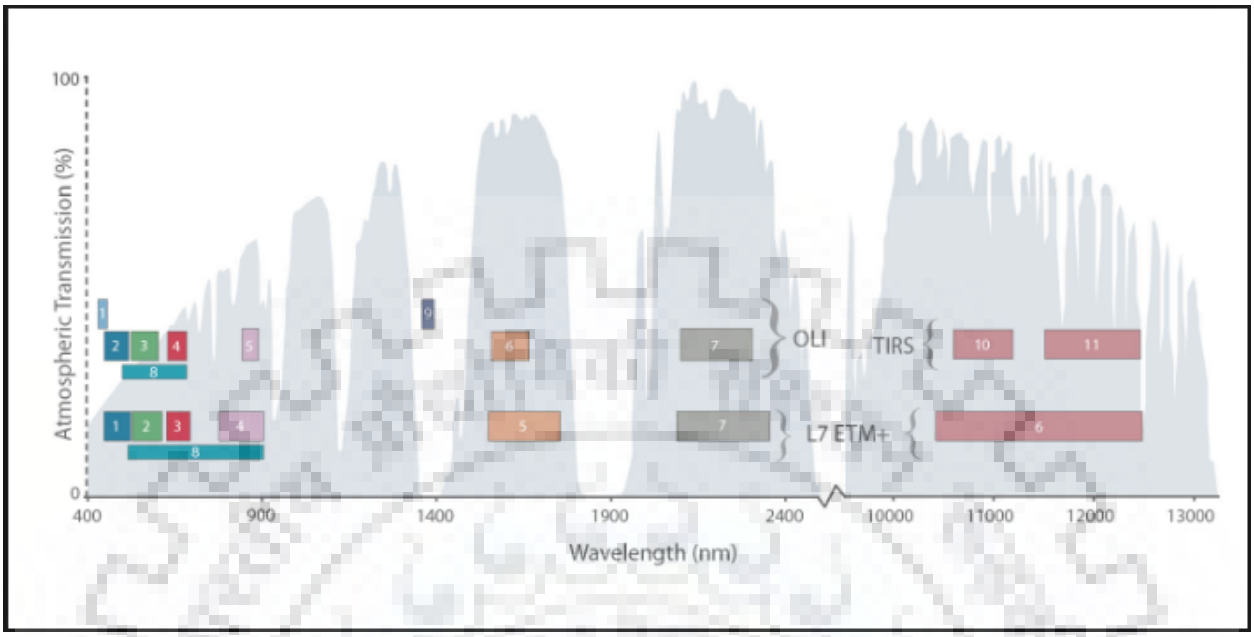

Figure 2.5. Comparison of OLI and TIRS instruments vs. Landsat 7 ETM+ sensors band pass wavelengths

(Source: USGS, 2013)

Table 2.1. Processing parameter for Landsat8 standard data products

Product Type	**Level 1T (terrain corrected)**
Data type	16-bit unsigned integer
Output format	GeoTIFF
Pixel size	15 meters/30 meters/100 meters (panchromatic/multispectral/thermal)
Map Projection	UTM (Polar Stereographic for Antarctica)
Datum	WGS 84
Orientation	North-up (map)
Resampling	Cubic convolution
Accuracy	OLI: 12 meters circular error, 90% confidence
	TIRS: 41 meters circular error, 90% confidence

All orthorectified data products (standard level -1) which are generated using Landsat 1 to Landsat 7 are consistent with Landsat 8 data products, by quantizing and calibrating scaled digital numbers (DNs) which represent data acquired by OLI and TIRS instruments (multispectral image

data). The 16-bit delivered format of the products (OLI and TIRS products) are rescaled to the TOA radiance and/or reflectance by resorting to the metadata file that provides radiometric rescaling coefficients. TIRS products are converted to the at-satellite brightness temperatures by extracting the thermal constant coefficients from metadata file. The spatial resolution is an important aspect of viewing a satellite image, but the difference in reflected sunlight by various earth surface objects employed to detect features, the targets are less appreciated. Landsat 8 facilitates further analysis in future thanks to its thermal and multispectral bands, also provides continuity to the anterior sensors.

Table 2.2. Landsat8 bands properties and applications

Landsat8 Sensors	**band**	**Band name**	**Wavelength (um)**	**Resolution (m)**	**Applications**
Operational Land Imager (OLI)	1	Coastal/Aerosol	0.433-0.453		Costal and Aerosol studies
	2	blue	0.450-0.515		Bathymetric mapping, differentiate vegetation from soil, and coniferous vegetation deciduous
	3	green	0.525-0.600		Emphasizes peak vegetation which is useful for assessing plant vigour
	4	red	0.630-0.680		Discriminates vegetation slopes
	5	NIR	0.845-0.885		Emphasis shorelines and organic matter content
	6	Shortwave Infrared (SWIR)1	1.560-1.660		Discriminates moisture content of the soil and organic matter: penetrates thin clouds
	7	Short-wave Infrared (SWIR)2	2.100-2.300		Improved moisture content of the soil and vegetation and thin clouds penetration
	8	panchromatic	0.500-0.680		Sharper image definition
	9	Cirrus	1.360-1.390		Improved cirrus detection and clouds contamination
Thermal Infrared Sensors (TIRS)	10	Long-wave Infrared (LWIR)1	10.30-11.30		Estimation of the soil moisture and thermal mapping
	11	Long-wave Infrared (LWIR)2	11.30-12.50		Improved thermal mapping and estimated soil moisture
	BQA	Quality assessment			Quality assessment for each pixel in the scene

2.3.4 Remote sensing applications for water quality assessment

Many researchers have used either bivariate regression or multiple regression to assess water quality from remote sensing techniques. It was observed in the published literature that instead of R^2 values, more importance was attached to Pearson correlation coefficients, R and Significance values being statistically sound. Forrer (2012) has employed LANDSAT 5 to assess water quality variables (TSS and *Chl-a*) of BANHEAD RESERVOIR OF THE BLACK WARRIOR RIVER and found that TSS was strongly correlated with B_3 to Sig* value of 0.008 63 (<0.05 p value) and R of 0.63. The TSS values ranged from 4-11 mg/l during the time under study. *Chl-a* was correlated with B1/4 to Sig* value of 0.007 and R of -0.77 percent. The *Chl-a* values ranged from 2-8mu/l. Nas (2004) and Wang (2006) stated that for water bodies which are not too much polluted, band ratios seem to be suitable for WQPs retrieving using remote sensing techniques. Jangan (2015) assessed Korean lake WQPs (TSS, CHL, TP and TN) employing Landsat 8 images and found that TSS, TP and *Chl-a* were correlated with band ratio (B2/4) to a Sig* of 0.01 and R of -0.71, -0.52 and -0.66 respectively.

Table 2.3. Multi and Bivariate Regression Models for remote sensing applications

Jangan (2015)	**Multivariate**		
WQPs	Regression equation	R	**Sig***
TSS	11.80 - 50.608*B_1 + 14.58*b4 - 4.7*B_4/2	-0.71	**0.01**
TP	0.06 + 0.041*b2-0.209*b4 + 0.003*B_4/2	-0.52	**0.01**
Chl-a	49.057 + 63.83*b2 - 236.05*B_4/2	-0.66	**0.01**
Forrer (2012)	**Bivariate**		
WQPs	Regression equation	R	**Sig***
TSS	0.308 + 23.574*B_3	0.63	**0.008**
Chl-a	1.019 - 0.437*B_1/4	-0.77	**0.007**

CHAPTER THREE

STUDY AREA AND METHODOLOGY

3.1 Study area

Lake Tumba is located 0 degree 45'S, 18 degrees 0'E in Equateur province in DRC, and drains north to Congo River. Lake Tumba is the second largest lake among all Congo basin's lakes. The largest lake Mai-Ndombe lies just South of lake Tumba. Lake Tumba is a shallow lake with a mean depth of about 3 m (Mputu, 2013). The area covered by the lake is about 765 Km^2 and may vary with seasons (Zanga, 2013). The lake is linked to Congo river via Irebu channel, through which water flows out or into the lake depending on flood levels. This water body harbors about 114 kinds of fish and constitutes a reservoir of important fisheries (FAO, 2012). The lake lies at the center of the Tumba-Ngiri-Maindombe area, designated wetland of international importance by the Ramsar convention in 2008.

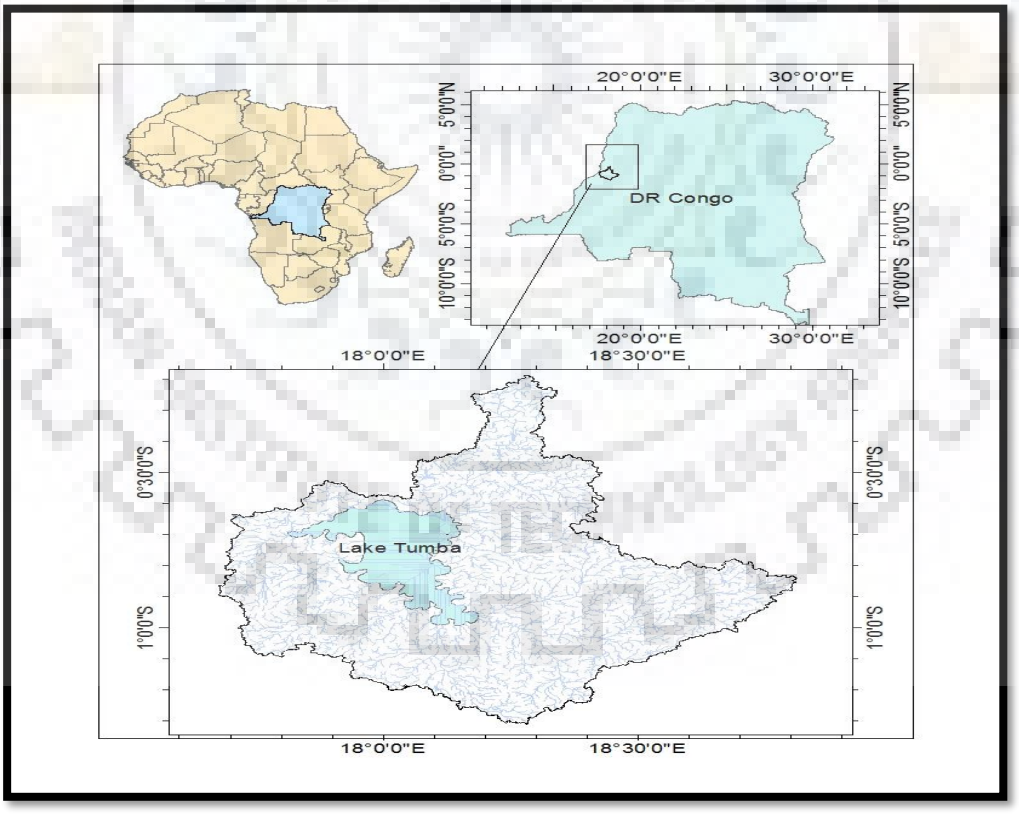

Figure 3.1. Study area delineation

3.1.1 Climate

Tropical and wet climate essentially dominates the ecoregion. Average annual temperature is approximately 25.C, min. and max. daily temperatures are 21.C and 31.C respectively (Hughes and Hughes 1992). The ecoregion receives an average of 1,800 mm of rainfall each year. October and November are two months that register highest rainfall, with 200 to 220 mm per month, followed by February and April, with 170 to 200 mm/month. July only registers 70 mm rainfall (Hughes and Hughes, 1992).

3.1.2 Freshwater Habitats

Situated on low slope, the lake Tumba records flood almost all the year. The small blackwater forest streams that flow the surrounding, inundated swamp into the lake are the main source of its nutrients. (Lévêque, 1997). The pH of the lake water is low due to water charged in carbon coming from the forest, ranging from 4.0 - 4.9 (Leveque, 1997; Brummett and Teugels, 2004; Thieme *et al.,* 2005 and Stiassny and Hopkins, 2007). Many islands are found within the Lake, and the mouths of some inflowing streams contain small deltas (Hughes, 1992). The la lake Tumba is shallow one, with depth being only 3 to 5 m, and the max depth being 8 m. DO is substantial in whole lake during the entire year due to frequent churning of the waters by strong winds. Irebu Canal allows lake Tumba waters to flow into the Congo River, but during high flood and floodwaters, the direction through the canal reverses from the Congo river entering the lake Tumba (Hughes, 1992).

Mats of *Echinochloa pyramidalis* and *Panicum parviflorum, Jardinea congoensis* and *J. gabonensis* produce in beds along the lake's edges and are occasionally interrupted by thickets of *Cyrtosperma senegalense* and *Rhynchospora corymbosa*n in calm cove waters. Sometimes these thickets freely drift and break off. The area along the shores which are minimally exposed at periods of low water flow are subject of swamp forests growth. During high water flow, these forests may be submerged up to 4 m in depth (Hughes, 1992).

3.1.3 Fish fauna

107 fish species were reported from lake Tumba (Hughes, 1992). Ecologically, the lake Tumba is similar to Lake Mai-Ndombe and both lakes are connected by inundated swamps during

the rainy season. The species like *Clupeocharax schoutedeni, Tylochromis microdon.* Mormyrids, clariid and bagrid catfishes, characoids, clupeids, rivulins, and cichlids which are purely lacustrine fishes do not move between these two lakes, only swamp-adapted fishes freely enter the lake Mai-Ndombe and vice-versa. Cichlidae and Clariidae are the two dominating fish families. *Nannothrissa parva, one of three clupeids* species inhabiting the lake is known only from Tumba, the Oubangui, and the upper Congo rapids. Congo river behaves like a canal during high floods, through which some species of fish enter the lake Tumba. (Hughes, 1992).

3.1.4 Other noteworthy fishes

Open waters of the lake harbor shoaling fish *(Barbus and Microthrissa)* and feed on small plankton (Hughes, 1992). The pelagic zone is inhabited by *Odaxothrissa losera* which feeds on small fish. The fish inhabiting near-shore areas of vegetation get their food from Insects and detritus. *Phago boulengeri* eats the fins of other fishes (Hughes, 1992).

3.1.5 Other aquatic biotic species

The vegetation near the lake Tumba banks serve as a refuge place for a large number of aquatic frogs and tadpoles (Hughes, 1992). Only 12 species of frogs are the most known relying on the lake. Two of them are endemic (*Cryptothylax minutus* and *Phlyctimantis leonardi*), which belong to the same family, *hyperoliidae*. The ecoregion also abounds many large aquatic reptiles and mammals. *Hippopotamus amphibus* is present but rare. *Crocodylus cataphractus* and *C. niloticus* are the two kinds of crocodile that occur in the lake (Hughes, 1992). Several piscivorous snakes inhabit Tumba landscape. The ecoregion abounds many kinds of bird which are similar to those of lower Congo River region. The African openbill (Anantomus lamelligerus). The pink-backed pelican (*Pelecanus refuscens*), and ducks (Anasspp.) inhabit the ecoregion (Hughes, 1992).

3.1.6 Ecological phenomenon

Allochthonous suspended biomass from the surrounding forests constitutes the mineral content, which serve as the food chain of the lake Tumba (Beadle, 1981). August and September are the two months between which most fish species spawn. During the high flood, these fish species move many of kilometers upstream and enter flooded forest to feed and breed (Lévêque, 1997).

3.2 Methodology for water quality monitoring and analysis

3.2.1 Water sampling

The lake water sampling for this study was conducted in the months of September and October 2018 during 3 days considering the large area of the lake. The polyethylene bottles used for water sampling were labeled, cleaned with nitric acid and rinsed twice with distilled water. At the sampling site, the bottles were rinsed three times with water to be sampled. The geographic coordinate of each sampling point was taken using a GPS receiver. The field sampling was conducted at 18 (eighteen) representative points for both September and October monitoring in the different parts of the lake, except the portion covered by vegetation. DO and pH were analyzed at the field itself, using DO meter and pH meter. All the samples were stored with ice packs and shipped to Agricultural Engineering Sciences Lab for analysis.

Table 3.1.Sampling points coordinates for September monitoring

Num	Sample names	X	Y	Sampling Depth(cm)
1	Village Tondo	180103.46	9909284.77	15
2	River tondo	180179.24	9911280.47	15
3	Village bikoro	180733.23	9919727.41	15
4	Inflow bikoro	177608.92	9929758.97	14
5	Village lokongoli	173565.99	9896011.66	14
6	Inflow lokongoli	171381.80	9896543.73	15
7	Inflow nkoso	166337.35	9903580.98	15
8	Village ikoko-bonginde	174159.99	9929015.20	14
9	Village bikoro1	179057.01	9918573.52	14
10	Village tondo1	178921.58	9908425.63	14
11	Inflow village kolo	178532.09	9890499.58	15
12	Lac_surface_pts1	160515.04	9910987.34	14
13	Lac_surface_pts2	163538.03	9907869.00	14
14	Lac_surface_pts3	168700.29	9911554.58	14
15	Lac_surface_pts4	170983.00	9916222.00	15
16	Lac_surface_pts5	167126.00	9921509.00	14
17	Lac_surface_pts6	161024.88	9927756.90	14
18	Lac_surface_pts7	155713.68	9926239.38	14

Table 3.2. Sampling points coordinates for October monitoring

Number	Sample names	X	Y	Sampling depth (cm)
1	village Tondo	180105.00	9909284.80	15
2	river tondo	180171.40	9911286.50	15
3	village bikoro	180738.30	9919732.43	14
4	inflow bikoro	177602.13	9929751.71	14
5	village lokongoli	173560.93	9896012.16	15
6	Inflow lokongoli	171385.81	9896547.71	15
7	Inflow nkoso	166335.34	9903581.95	15
8	village ikoko-bonginde	174162.22	9929018.40	15
9	village bikoro1	179058.31	9918576.54	14
10	village tondo1	178924.58	9908422.33	15
11	inflow village kolo	178534.09	9890494.58	15
12	lac_surface_pts1	160517.10	9910985.59	14
13	lac_surface_pts2	163534.18	9907872.00	14
14	lac_surface_pts3	168703.18	9911554.58	14
15	lac_surface_pts4	170988.00	9916228.00	15
16	lac_surface_pts5	167121.00	9921519.00	15
17	lac_surface_pts6	161028.19	9927752.90	15
18	lac_surface_pts7	155713.11	9926225.57	15

3.2.2 Laboratory Analysis

The laboratory analyses were carried at the laboratory of water quality of Agricultural Sciences. The water quality parameters included Turbidity, Chlorophyll-a, Total phosphorus and Total suspended solids. In the laboratory, turbidity and TSS were analyzed according to standards procedures for the examination of water and wastewater provided by APHA (1992). *Chlorophyll-a* and total phosphorus were analyzed following the standard procedures provided by EPA.

3.2.2.1 Turbidity

The samples were gently agitated. The mixed samples were poured into a cell and immersed in an ultrasonic bath for 1 to 2 seconds after applying vacuum degassing to cause complete bubble release. Then the turbidity values were directly read from the instrument display (APHA, 1992).

3.2.2.2 TSS

The samples were well mixed and filtered using a standard, pre-weighed, glass-fiber filter. The residues were dried at a temperature of 103-105^{0}C. The increase in the filter's weight indicates the total suspended solids concentration (APHA, 1992)

3.2.2.3 *Chlorophyll-a*

The method 445.0 of EPA was used to determine *Chl-a* concentration (Arar and Collins 1997). The method uses fluorescence detection to estimate *Chl-a* in fresh and marine water (Arar and Collins 1997). The samples were concentrated and filtered with a low vacuum through a fiber filter. The filters were tearing into small strips and incubated for 1,080 minutes in acetone prepared at 90% in the freezer and agitated many times (NSF 2004). The filter slurry was centrifuged at 675 g for 15 minutes to clarify the solution. Before and after acidification to 0.003 N HCL, the fluorescence of an aliquot was then measured by adding 0.1 N HCL. To estimate *Chl-a* concentration in the extracted sample, sensitivity calibration factors were finally applied (Arar and Collins 1997).

3.2.2.4 Total Phosphorus

The method 365.4 of EPA was used to determine total phosphorus concentration. Water sample was heated for 2.5 hours in the presence of H_2SO_4 (sulfuric acid). Dilution to 25 mg with distilled water and cooling of the residue were done. The residue was then placed on the Auto Analyzer for phosphorus determination (EPA, 1974).

3.3 Processing of remote sensing data

3.3.1 Data availability

Two Landsat 8 OLI images (Path: 180 and Row: 61) were used in this particular study in view of assessing lake Tumba water quality. The images were acquired for 19th September and 16th October 2018 during rainy season. Both images were downloaded from USGS EARTH EXPLORER and radiometrically corrected. The following figure describes the methodology used in this particular study.

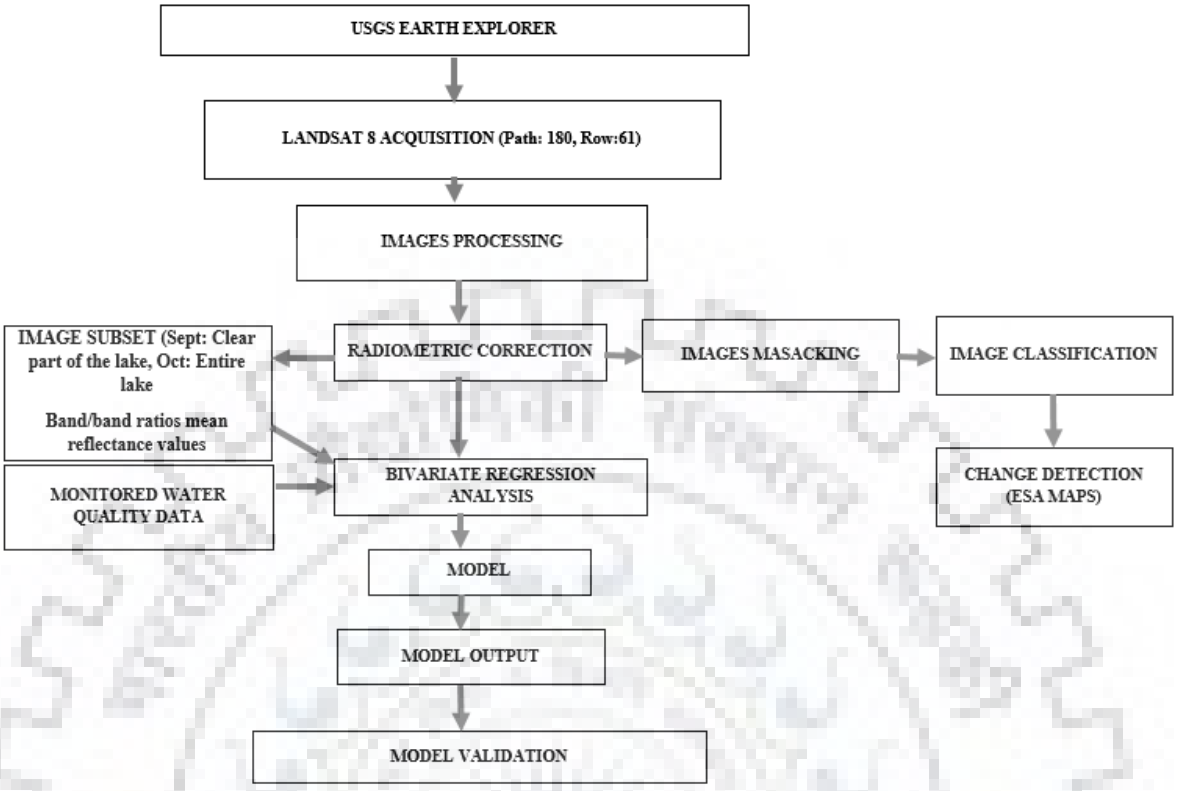

Figure 3.2. Methodology chart

3.3.2 Radiometric correction

To retrieval water quality variables from remote sensing techniques, radiometric correction is very crucial (hu *et al*., 2004) as atmospheric reflection, refraction and absorption of light affect the image (Chavez, 1988). Radiometric correction was performed to mitigate these noise from atmosphere and transform DNs (Digital Numbers) to the spectral reflectance values (Chavez, 1996). Dark object subtraction (DOS) algorithm in QGIS has been applied to transform DNs to at sensors reflectance values (Skirvin, 2000). IBDOS model prosed by Chavez (1996) was selected for the same. The model variables are reprised below:

$$\rho\lambda = (Lsatrad - Lhaze\ 1\%)\ \pi * \frac{d2}{Eo\lambda} * cos\theta s * TAUv$$

Where ρλ = surface water reflectance, d = gap between earth surface and sun (in astronomical units),

$Lsat_{rad}$ = sensor spectral radiance ($Wm^{-2}sr^{-1}\mu m^{-1}$).

$Lsat_{rad} = M_{L*} Q_{cal} + A_L$

where ML and AL are the band-specific multiplicative and additive factors respectively, contained in metadata file, Qcal = Digital Number value

$$L_{haze\ 1\%rad} = L\lambda_{min} - L\lambda,\ 1\%$$

Where $L\lambda_{min}$ is sensor's min spectral radiance, $L\lambda$, 1% is the band radiance, supposed to have 1% of reflectance

$$L\lambda,\ 1\% = 0.01 * E_o\lambda * \cos\theta / d^2 * \pi$$

Where $E_o\lambda$ = external atmospheric solar irradiance, θ = zenith angle of the sun, TAU_v = atmospheric radiance transmission from earth surface to the sensor.

After radiometric correction, image subsetting was performed using ERDAS Imagine software. Often, the images from EARTH EXPLORER contain areas too vast than the area of interest. Image subsetting was applied to only extract the area of interest (lake Tumba). For september image, not the entire lake was clear, some part was impacted by clouds and only the clear portion of the lake (contenaining 9 sampling points out of of 18) was extracted to be used in water quality analysis. The october image was also impacted by clouds, but not within the lake. The entire portion of the lake was subsetted for water quality analysis.

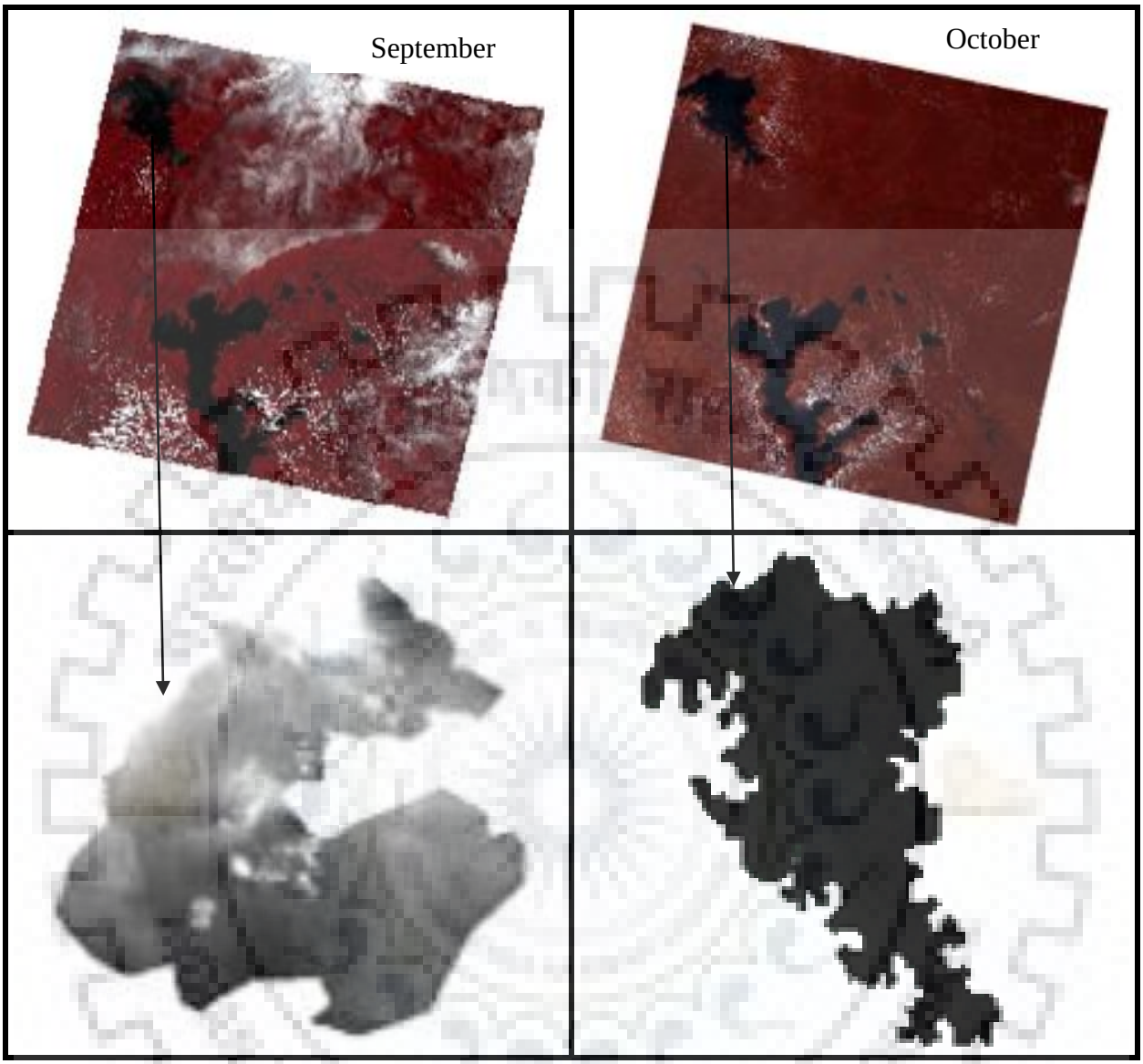

Figure 3.3. Images processing

3.3.3 Image classification

Mosaicking operation was performed before image classification to generate one image that represents whole catchment (lake Tumba catchment). 4 image tiles geo-referenced, containing the same map and projection information with the same number of layers were joined together (mosaicking). Often, the images used for classification contain areas too vast than the area of interest. Image sub setting was applied to extract only the lake Tumba catchment. Image sub setting not only rules the excess data in the image file out, but it also facilitates the processing due to reduced amount of the data to process (ERDAS, 1999).

Supervised classification using MLC was performed. Areas to represent each land cover class in the map were selected (training sites). It is just the samples of image's elements that represent particular land cover class. They commonly represent identified or detectable samples to be mapped as land cover classes (ERDAS, 1999). They are pixels that represent what is recognized as a discernable pattern, or potential land cover class. On-screen digitizing of selected areas for each identified land cover on colour composite was performed to generate these training sites. An estimation classification was performed to evaluate the selected training pixels (ALARM command). This process helps to pre-classify the image data and select certain places among chosen land cover classes from where the occurrence of error may be possible.

In fact, it is a visual tool that gives an overview of where the classes will be assigned in the image and whether additional classes are required. Training samples were refined based on the analysis of outcome until an acceptable outcome was attained. The purpose was to generate classes that resemble well to the earth's surface features. The digital image classification helps furnishing effective, compatible and repeatable routines to map vast areas (Kashaigili, 2006). The images characteristics like color, pattern, and texture were used to convert the image into land covers for visual interpretation. This operation involved enhanced image colour composite. The following classes were used: water bodies, Forest, Wetland, settlement and Agriculture.

3.3.4 Change detection

Missing the free cloud images of earliest years, ESA classified map was used for this purpose**.** Assessment of the change detection is generally useful as it helps identifying Changes that are developing or happening over a specific period in a defined place (Yeh et al., 1996). The two most categories of algorithms used in change detection are: (a) pixel-to-pixel comparison of multi-temporal images before image classification, and (b) post-classification comparison (Jensen, 1996).

In our case, we resorted to a post-classification comparison in view of assessing LULC changes over a period of 15 years. It is a suitable method (Jensen, 1996; Mundia and Aniya, 2006) of comparing data obtained in different seasons and from different references. This method has an advantage to overcome some complications linked to the analysis of images obtained in different seasons and from different references (Yuan et al., 2005; Coppin et al., 2004; Alphan, 2003). The LULC changes are effective using this approach (Wickware and Howarth, 1981); as it helps

quantifying changes that take place. The only limitation that can be evoked in this method is that, if the accuracy of each land cover class is wrong, the generated maps will also be wrong (Yuan et al., 2005; Zhang et al., 2002). This process enables changes identification using change detection matrix by comparing some independent classified images on the basis of pixel-by-pixel (Yuan and Elvidge, 1998). The change matrix generates a thematic layer holding an independent class for each coincidence of classes in multi-date dataset.

3.3.5 Change detection analysis

The following formulas helped to compute LULC change detection (Jensen, 1996) in lake Tumba catchment:

$$\%\ of\ cover\ change = \frac{Area\ i\ year\ x - Area\ i\ year\ x+1}{\sum Area\ i\ year\ x} * 100$$

$$Annual\ rate\ of\ change = \frac{Area\ i\ year\ x - Area\ i\ year\ x+1}{\text{tyears}}$$

$$\%\ Annual\ rate\ of\ change = \frac{\text{Area i year x} - \text{Area i year x} + 1}{\text{Area i year x} * \text{tyears}} * 100$$

Where $area_{i\ year\ x}$ = area of cover at the first date, $Area_{i\ year\ x+1}$ = area of cover at the second date, $\sum area_{yearx}$ = total cover area at the first date and t_{years} = period in years between the first and the second scene acquisition dates

3.3.6 Correlating water quality variables and reflectance

The radiometrically corrected Landsat 8 images were utilized for remote water quality assessment in this research. On the basis of UTM coordinates determined with a GPS device, the sampling points were located on the image and extracted for use in correlation and regression analysis. A 3x3 window around each sampling pixel was used for pixel values extraction (Brivio *et al*., 2001; Wang *et al*., 2005; Zhou *et al.*, 2006).

To determine how strong is the model, a Pearson correlation matrix was performed for both datasets. Bivariate linear regression modes were developed to check the correlation between measured water quality variables concentration, bands and band ratios mean reflectance values. Mean reflectance values were extracted from bands and band ratios of both images to be used as predicting variables in regression analysis. Blue (Band1), green (Band2), red (Band3) and near

infrared (Band4) bands have been selected to analysis correlation between dependent variables (TSS, Tb, TP, *Chl-a*) and independent variables (Peters and Dekker, 1993). Band ratios mean reflectance values of the 9 points found within the clear part of the lake for September image were used in regression model. Dependent variables that were utilized in this particular study include TSS, TP and *Chl-a*. Mean reflectance bands and band ratios values were used as independent variables.

The statistical analysis was performed using EXCEL software. The choice of regression model equation to estimate all water quality variables was made based on correlation coefficients, significance value of each model developed, actual vs. predicted water quality values and apparent analysis of the generated maps.

CHAPTER FOUR

RESULTS AND DISCUSSION

4.1 General water quality status of the lake Tumba

Table 4.1. Monitored water quality parameters for both September and October 2018

lab				in situ		
Chl-a (mug/l)	Tb (NTU)	TP (mug/l)	TSS (mg/l)	PH	DO (mg/l)	Temp. (0C)
0.034	11.126	2.398	1.587	4.8	5	24
0.036	10.121	2.111	2.112	4.8	5	24
0.039	12.987	2.371	2.301	4.9	5.1	24
0.038	9.985	2.318	1.765	4.7	5.1	24
0.034	11.432	2.998	1.821	4.8	5	24
0.035	11.876	2.837	1.221	4.8	5	24
0.033	8.983	2.362	1.962	4.9	5	24
0.029	9.659	3.054	2.103	4.8	5	24
0.031	10.511	2.951	2.096	4.7	5	24
0.034	10.651	2.437	1.296	4.7	5.1	24
0.025	9.111	3.453	2.761	4.9	5	24
0.02	8.866	1.651	2.436	4.8	5	24
0.019	7.254	1.567	2.334	4.9	5.1	24
0.019	7.312	1.763	2.341	4.9	5	24
0.02	7.121	1.742	2.111	4.8	5	24
0.018	7.324	1.699	2.332	4.9	5.1	24
0.018	7.431	1.691	2.342	4.9	5	24
0.018	7.323	1.751	2.311	4.9	5	24

lab				in situ		
Chl-a (mug/l)	Tb (NTU)	TP (mg/l)	TSS (mg/l)	PH	DO (mg/l)	Temp. (0C)
0.036	11.262	2.987	1.623	4.9	5	24
0.037	11.125	2.234	2.149	4.9	5	24
0.039	11.887	2.865	2.34	4.9	5	24
0.04	11.459	2.518	1.805	4.8	5	24
0.038	11.333	3.548	1.859	4.9	5	24
0.037	11.876	2.137	1.258	4.9	5	23
0.036	12.911	2.132	1.998	4.9	5	23
0.037	11.612	2.554	2.14	4.8	5.1	24
0.035	12.321	3.001	2.131	4.8	5.1	24
0.036	10.881	2.783	1.332	4.9	5	23
0.026	10.138	2.888	2.787	4.9	4.9	23
0.035	10.865	2.151	2.471	4.9	5	23
0.034	11.213	1.881	2.368	4.8	5	24
0.038	10.313	2.299	2.379	4.8	5	24
0.03	11.128	1.997	2.141	4.8	5	23
0.03	12.524	1.689	2.362	4.9	5	24
0.034	12.457	1.592	2.376	4.9	5	24
0.035	11.821	1.815	2.346	4.9	5	24

Table above shows the monitored water quality parameters for September and October 2018 conditions. In temperature, there is absolutely no variation during both September and October monitoring. From data which are available (Table 4.1), the variability of DO and pH is also negligible. The concentration of the monitored water quality parameters is too small, less than 10 mug/l for Total Phosphorus, and less than 8 mug/l for *Chl-a*. Thus, water quality of the lake Tumba can be classified as "Oligotrophic". These findings are supported by Chapman (1996) who stated for all lakes holding TP value not exceeding 10 mug/l and *Chl-a* value not exceeding 8 mug/l are Oligotrophic. The descriptive statistics for TSS, TP, *Chlorophyll-a* and Turbidity for both months are provided below.

Table 4.2. Descriptive statistics for September water quality parameters

Parameters	N	Max	Min	Mean	Std. Deviation
TSS (mg/l)	18	2.76	1.22	2.06	0.40
TP (mug/l)	18	3.45	1.57	2.28	0.58
Chlorophyll-a (mug/l)	18	0.04	0.02	0.02	0.007
Turbidity (NTU)	18	12.98	7.12	9.39	1.83

Table 4.3. Descriptive statistics for October water quality parameters

Parameters	N	Max	Min	Mean	Std. Deviation
TSS (mg/l)	18	2.79	1.26	2.1	0.39
TP (mug/l)	18	3.55	1.59	2.39	0.53
Chlorophyll (mug/l)	18	0.04	0.03	0.03	0.003
Turbidity (NTU)	18	12.98	7.12	9.39	1.83

The figures below show the equiconcentration contour maps, indicating the spatial variability of WQPs in the lake Tumba. Higher TSS concentrations were recorded at village Ikoko (2.761mg/l), inflow from bikoro village (2.4mg/l) and near village tondo (2.3 mg/l). Low concentrations were recorded at inflow from village nkoso (1.22mg/l), lake surface5 (1.82 mg/l) and at lake surface4 (2.1 mg/l). The highest concentrations of TP and *Chl-a* were recorded at lake surface5 (3.5 mug/l), inflow from lokongoli village (3mug/l), village Ikoko (2.9mug/l), village lokongoli (2.8mug/l); and lake surface2 (0.038mug/l), lake surface1 (0.036mug/l), village nkoso (0.035mug/l), village lokongoli (0.034 mug/l) respectively. The low concentrations of TP and *Chl-a* were recorded at inflow from village kolo (1.592mug/l), village tondo (1.815mug/l), village bikoro (1.881mug/l), and village tondo (0.018mug/l), village bikoro (0.019mug/l), village Tondolo (0.02mug/l) respectively.

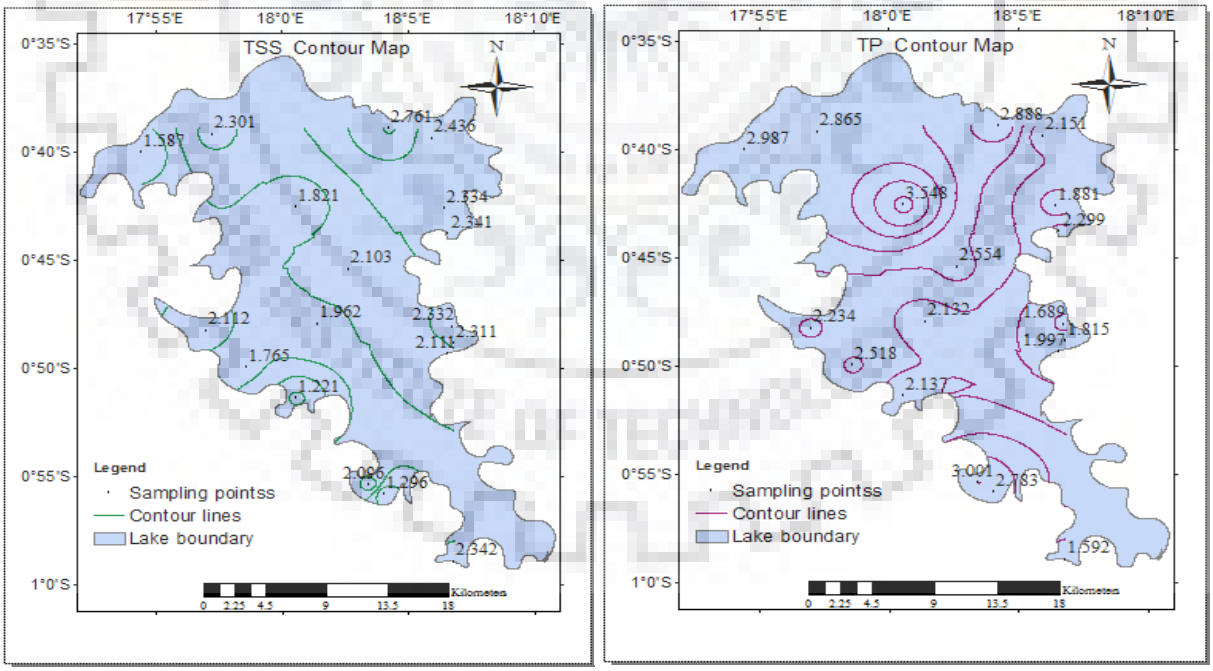

Figure 4.1. Equiconcentration contour maps of TSS and TP

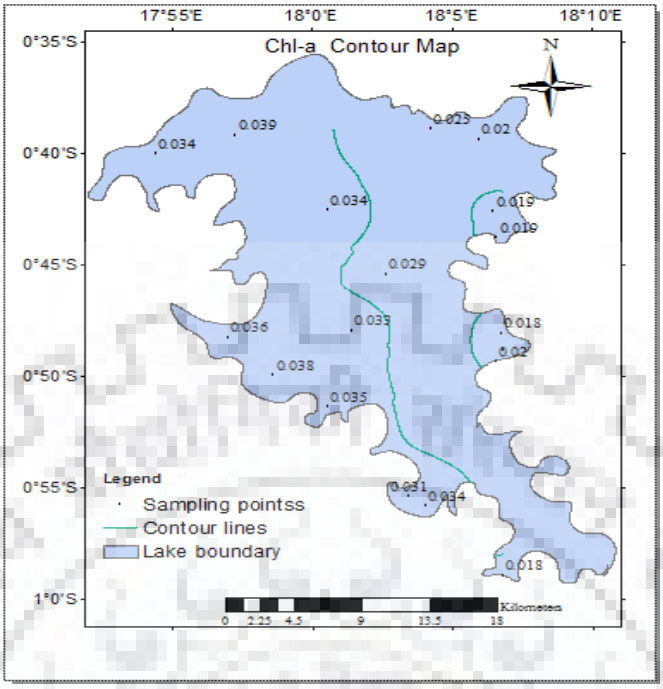

Figure 4.2. Equiconcentration contour map of *Chl-a*

4.2 Land Use and Cover results

LULC map includes lake Tumba watershed (Figure 4.3). The study area surrounding the watershed consists generally of flooded forest (83.86%). Water bodies also occupy an important portion in watershed (10.32%), followed by agriculture, wetland and settlement.

Table 4.4. LULC areas and percentage of covered area

Land Use Classes	Km^2	% Cover
Forest	6118.01	83.86
Water bodies	752.97	10.32
Agriculture	360.96	4.94
Wetland	35.56	0.48
Settlement	27.24	0.37

Table 5 lists the total area. The settlements that are present in lake Tumba catchment area have a low density (0.37%) considering the total covered area (7,294.77 sq. km). Still, this component may be considered important as Emmerth and Bayne (1996) and Wahl (1997) earlier stated that small towns may also serve as important source of NPSP.

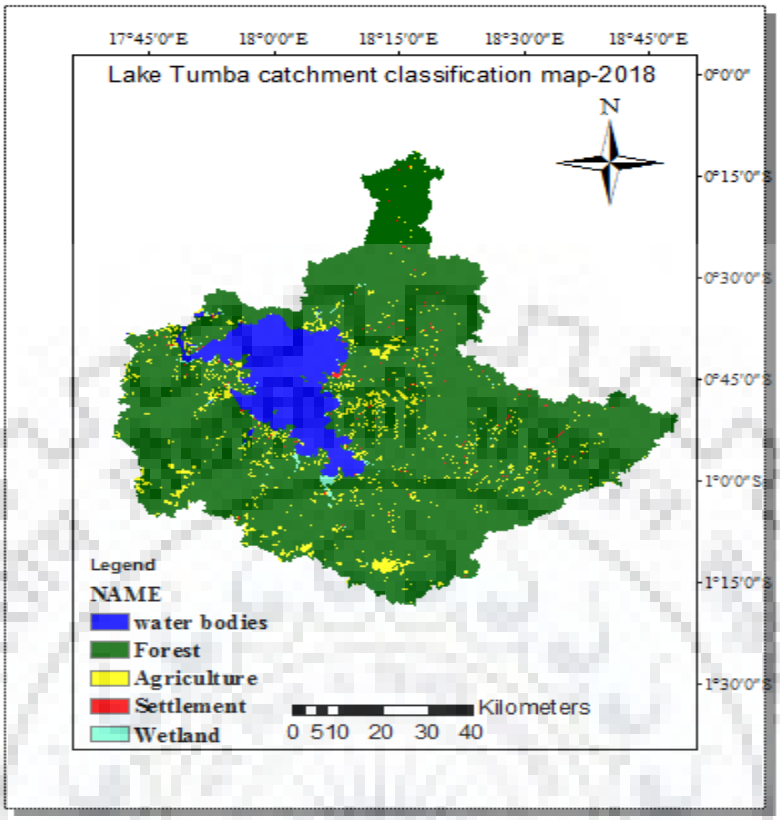

Figure 4.3. LULC Classification map

4.3 Change detection results

Table 4.5 shows the covered area for each class from 2000-2015. The percentage of coverage change and the change in area between 2000 and 2015 are shown in the table 4.6. The area (Km^2) covered by forest between two periods (2000 and 2015) was 5770.35 and 5756.58 (83.64 and 83.44%) respectively. The area decreased by 13.17 km^2 (0.20%) for this interval of period under consideration (2000 and 2015). The area covered by Water bodies was 741.15 and 736.65 Km^2 (10.74 and 10.68%), which decreased by 4.5Km^2 (0.07%) between 2000 and 2015 while agriculture increased by 16.65 Km^2 (0.24%). Wetland and settlement were covering an area of 13.68, 14.16 and 2.16, and 2.7 (0.20, 0.03, 0.21 and 0.04%) between 2000 and 2015, and increased by 1.08 and 0.54 Km^2 (0.02 and 0.01%) respectively. Annual rate of change (Km^2/year) for forest and water bodies has decreased by 0.92 and 0.30 Km^2 (0.02 and 0.04%) while agriculture area increased on an annual basis by 1.1Km^2 (0.30%). Wetland and settlement area also increased by 0.07 and 0.04 Km^2 (0.53 and 1.67%), annually.

Table 4.5. Covered area for each class from 2000-2015

	Agriculture	Forest	Settlement	Water	Wetland
2000	371.43	5770.35	2.16	741.15	13.68
2001	367.11	5774.31	2.16	741.51	13.68
2002	366.39	5775.57	2.16	740.97	13.68
2003	366.93	5775.03	2.16	740.97	13.68
2004	375.84	5765.94	2.16	741.06	13.77
2005	377.01	5763.93	2.16	740.52	14.31
2006	381.6	5762.25	2.16	738.45	14.31
2007	378.99	5764.68	2.16	738.63	14.31
2008	374.67	5770.71	2.16	736.83	14.4
2009	380.43	5765.04	2.16	736.65	14.49
2010	383.22	5761.8	2.16	737.1	14.49
2011	390.96	5753.97	2.25	737.1	14.49
2012	392.13	5753.34	2.43	736.38	14.49
2013	392.49	5752.89	2.52	736.38	14.49
2014	388.17	5756.58	2.61	736.65	14.76
2015	388.08	5756.58	2.7	736.65	14.76

Table 4.6. Change detection

Cover classes	2000		2015		Change in area (Km^2)	% of Change	Annual rate of change (km^2/year)	% Annual rate of change (% /year)
	Cover area (Km^2)	% cover coverage	cover area (km^2)	% cover coverage				
Forest	5770.35	83.64	5756.58	83.44	-13.77	-0.20	-0.92	-0.02
Water	741.15	10.74	736.65	10.68	-4.5	-0.07	-0.30	-0.04
Agriculture	371.43	5.38	388.08	5.63	16.65	0.24	1.11	0.30
Wetland	13.68	0.20	14.76	0.21	1.08	0.02	0.07	0.53
Settlement	2.16	0.03	2.7	0.04	0.54	0.01	0.04	1.67
Total	6898.77	100	6898.77	100				

Figures 4.4 - 4.8 show the trend of change in area for each class from 2000 to 2015

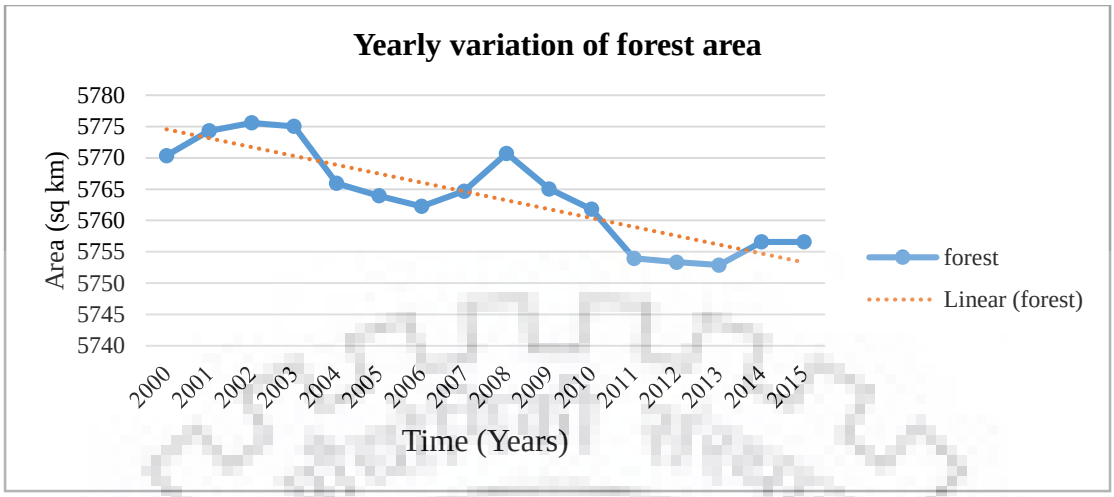

Figure 4.4. Trend of forest area variation

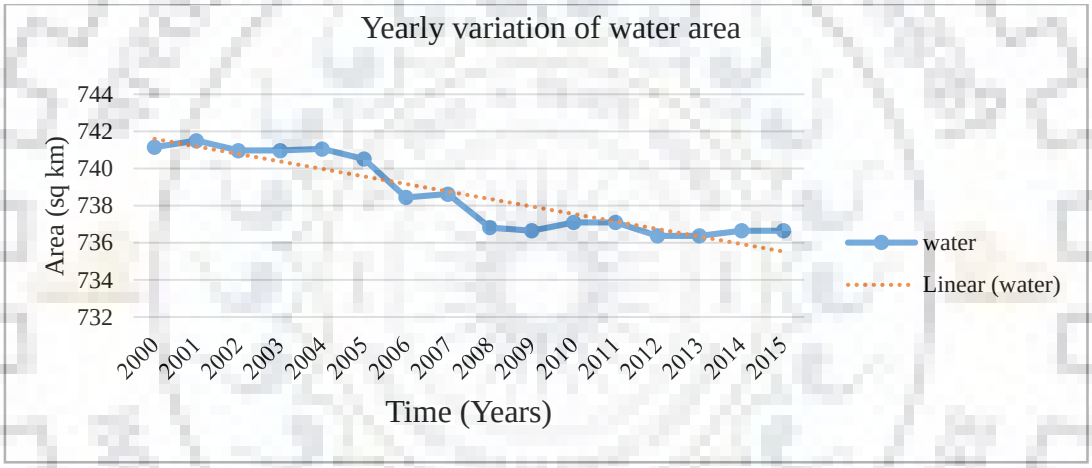

Figure 4.5. Trend of water area variation

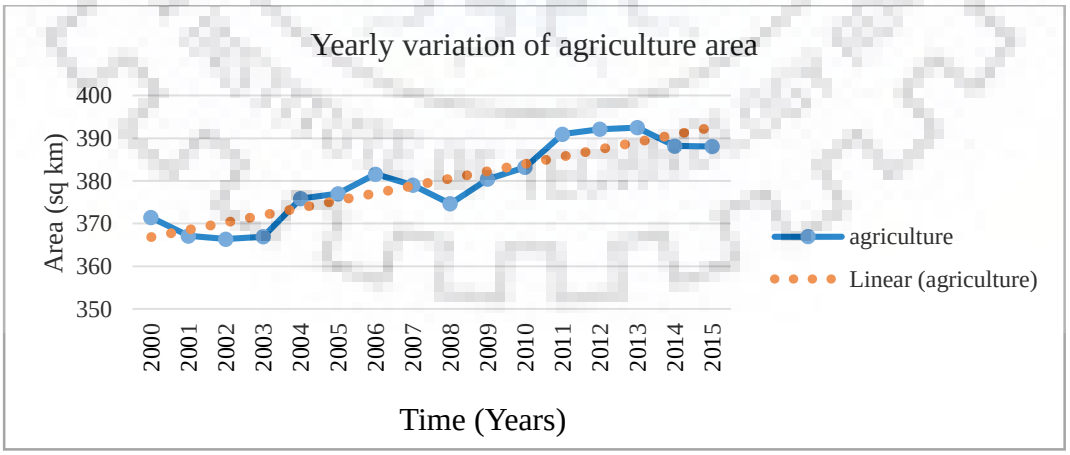

Figure 4.6. Trend of agriculture area variation

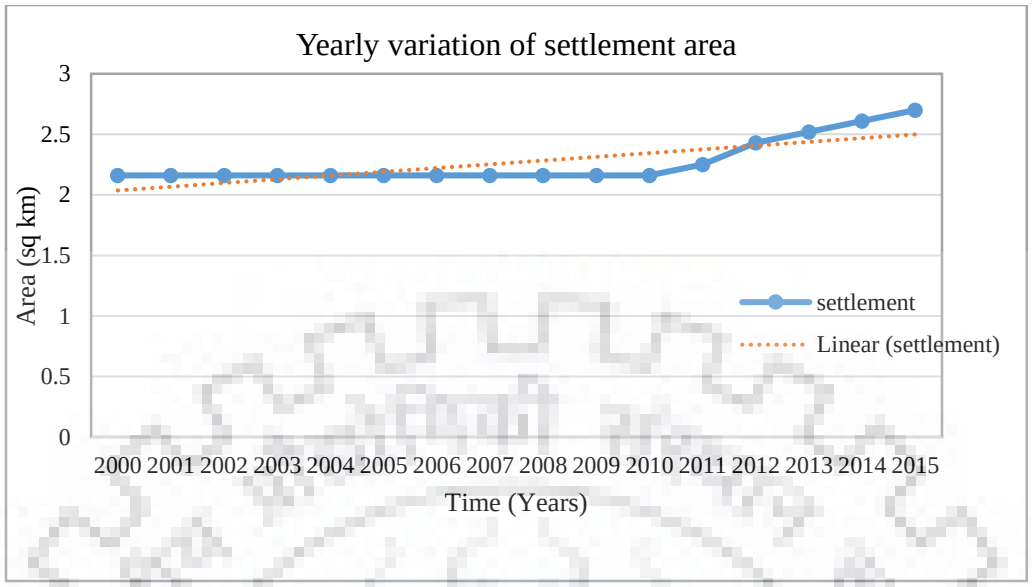

Figure 4.7. Trend of settlement area variation

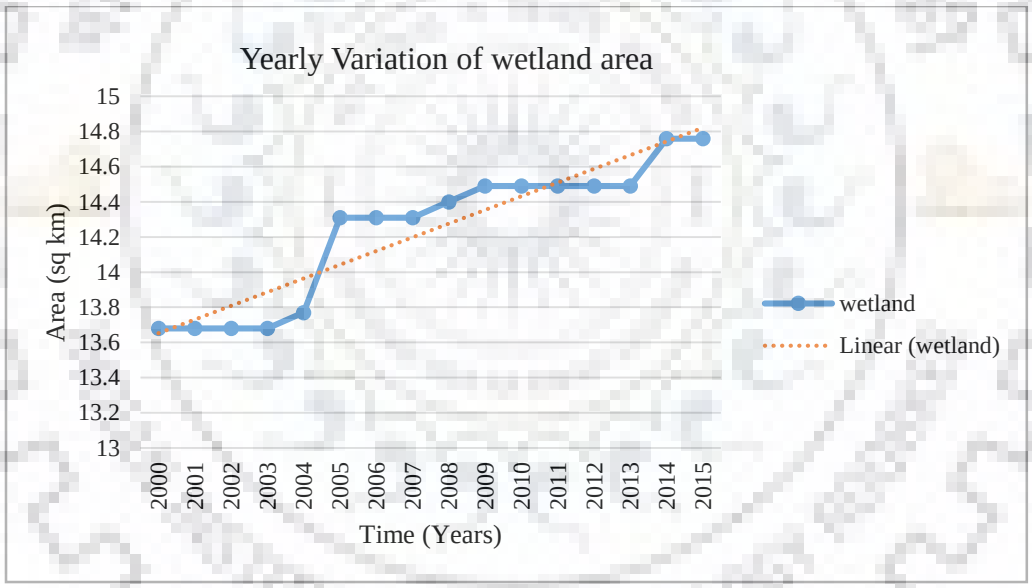

Figure 4.8.Trend of wetlands area variation

The figures 4.9 - 4.12 show the ESA LULC classified maps for an interval of 5 years

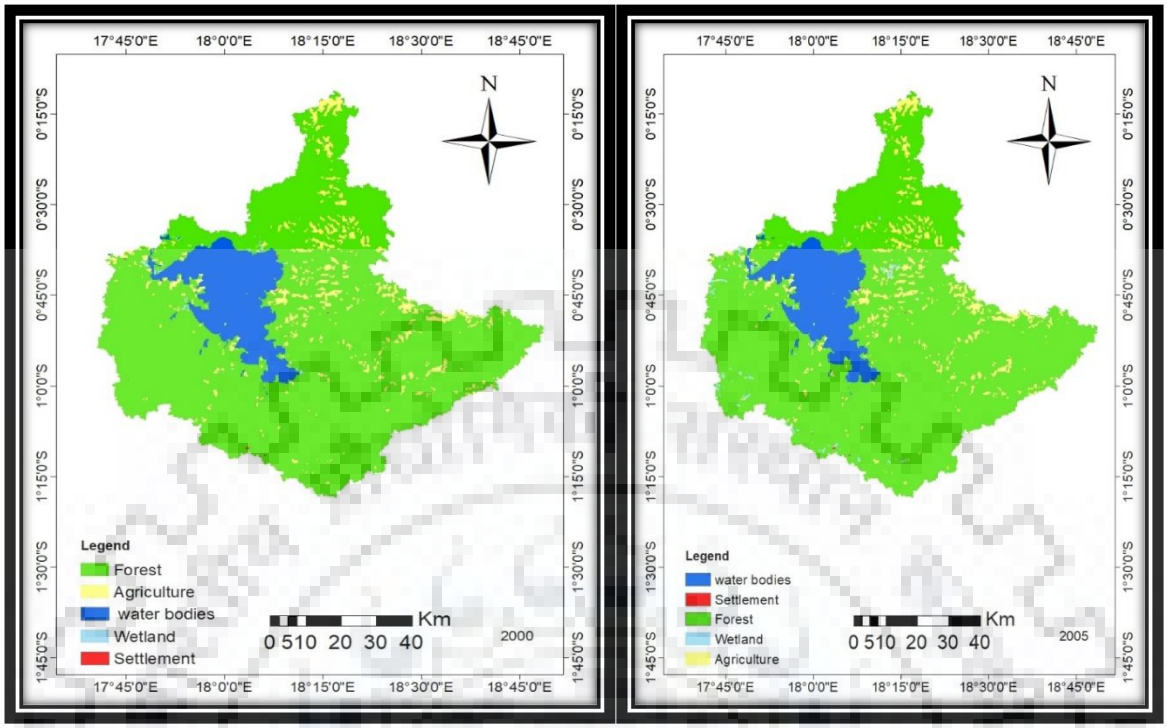

Figure 4.9. ESA LULC 2000 and 2005 maps

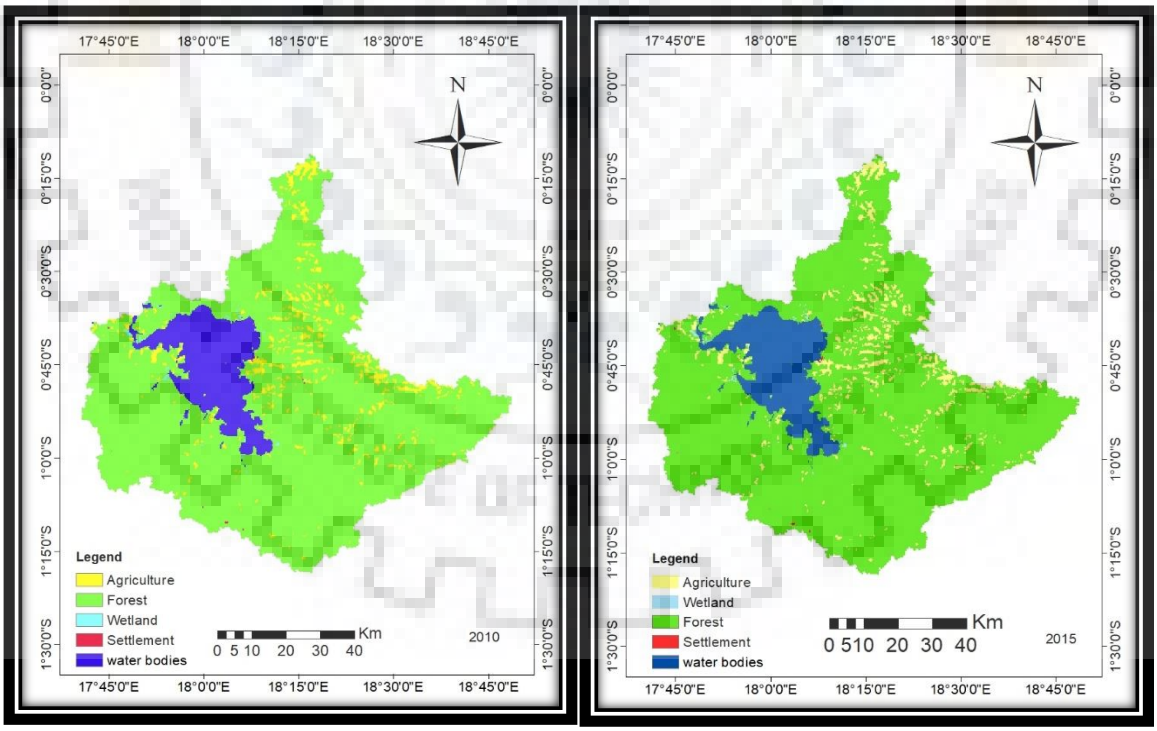

Figure 4.10. ESA LULC 2010 and 2015

4.4 Remote sensing aided water quality assessment for September 2018

4.4.1 Monitored water quality variables

Table 4.7. September TSS, TP, *Chl-a* and Tb concentrations

Sample	TSS (mg/l)	TP (μgl^{-1})	Chl-a (μgl^{-1})	Tb (NTU)
1	1.587	2.398	0.034	11.126
2	2.112	2.111	0.036	10.121
3	2.301	2.371	0.039	12.987
4	1.765	2.318	0.038	9.985
5	1.821	2.998	0.034	11.432
6	1.221	2.837	0.035	11.876
7	1.962	2.362	0.033	8.983
8	2.103	3.054	0.029	9.659
9	2.096	2.951	0.031	10.511
10	1.296	2.437	0.034	10.651
11	2.761	3.453	0.025	9.111
12	2.436	1.651	0.02	8.866
13	2.334	1.567	0.019	7.254
14	2.341	1.763	0.019	7.312
15	2.111	1.742	0.02	7.121
16	2.332	1.699	0.018	7.324
17	2.342	1.691	0.018	7.431
18	2.311	1.571	0.018	7.323

Table 4.5 shows the laboratory concentrations of TSS, TP, *Chlorophyll-a* and Turbidity found at the eighteen sampling points. Turbidity failed to show reasonably good correlation for bivariate linear regression model. Only three parameters (TSS, TP, *Chl-a*) were considered in this particular study, for both September and October dataset. The highest amount of TSS (2.761mg/l) was recorded near Inflow village Kolo. The highest amount of TP was recorded near the village Ikoko and lowest concentration was found near lake surface1. During September conditions, lake Tumba was not threated by algal bloom, apparently a reason why *Chl-a* and TP concentrations are low.

4.4.2 Correlating spectral reflectance and water quality variables

The Correlation between Landsat 8, 1-4 bands and band ratios derived reflectance values and water quality parameters (Total Suspended Solids, Total phosphorus and Chlorophyll-a) was estimated MS Excel. Table 4.8 lists band mean reflectance values for all 18 sampling points. The table 4.9 shows the Pearson correlation coefficients (r and Sg*) of September variables (TSS, TP and *Chl-a*). Different correlation coefficient values were recorded for each band/band ratios and water quality variables respectively.

Table 4.8. Mean band reflectance values for each sampling points

	Band1	**Band2**	**Band3**	**Band4**
1	0.045	0.03	0.04	0.03
2	0.03	0.02	0.02	0.02
3	0.042	0.03	0.03	0.03
4	0.087	0.07	0.07	0.01
5	0.038	0.02	0.03	0.02
6	0.12	0.10	0.11	0.15
7	0.037	0.027	0.03	0.04
8	0.038	0.027	0.03	0.03
9	0.039	0.028	0.03	0.03
10	0.04	0.03	0.035	0.04
11	0.075	0.06	0.06	0.08
12	0.037	0.028	0.03	0.04
13	0.04	0.03	0.03	0.03
14	0.04	0.03	0.03	0.04
15	0.035	0.02	0.026	0.02
16	0.04	0.03	0.03	0.03
17	0.037	0.025	0.02	0.02
18	0.03	0.02	0.02	0.03

No single band has correlation with any water quality parameters for September conditions. Band ratio B2/4 was however found to have strong correlation with TSS. TSS has a strong negative correlation with GNDVI also. *Chlorophyll-a* and TP were most highly correlated with band ratios b2/4 and R3/4. Surface water that contains more algae presents different spectral curves with absorption in green and blue regions. Maximum and peak reflectance are displayed in red and near infrared regions. (Han, 1997). *Chl-a* and TP were also positively correlated with NDVI.

4.4.3 Estimating TSS, TP and Chl-a during September conditions

Table 4.9. Pearson correlation coefficients between water quality parameters and various Landsat8 bands

	Band1	Band2	Band3	Band4	B1/2	B1/3	B1/4	B2/3	B2/4	B3/4	BNDVI	GNDV	NDVI
TS r	0.09	0.005	-0.02	-0.30	0.24	0.29	0.70	0.29	**0.79**	0.74	-0.70	-0.80	-0.75
*Sig**	0.8	0.9	0.94	0.41	0.53	0.44	0.03	0.43	**0.01**	0.02	0.03	0.01	0.02
TP r	-0.23	-0.15	-0.13	-0.13	-0.07	-0.07	-.54	-.04	-.70	**-.71**	0.54	0.70	0.71
*Sig**	0.54	0.69	0.72	0.72	0.84	0.84	0.12	0.91	0.03	**0.03**	0.12	0.03	0.03
Chl r	-0.27	-0.21	-0.21	0.08	0.03	0.08	-.50	0.17	-0.72	**-0.78**	0.50	0.72	0.78
*Sig**	0.47	0.58	0.57	0.82	0.92	0.83	0.16	0.65	0.02	**0.01**	0.16	0.02	0.01
Tb r	-0.3	-0.26	-0.28	-0.03	-0.10	0.18	-0.3	0.33	-.53	-.63	0.33	0.53	0.63
*Sg**	0.4	0.5	0.5	0.9	0.78	0.64	0.37	0.37	0.13	0.06	0.37	0.13	0.06

Extracted mean band ratios reflectance values were utilized to develop regression models for water quality variables (Total Suspended Solids, Total Phosphorus and *Chl-a*) estimation. Predicting and predicted variables include Landsat 8 band ratios and monitored water quality variables respectively. Table 4.10 shows the predicting power of the model (R^2) and the significance values (Sig*) band ratios. B2/4 was the band ratio holding the highest correlation with TSS. Dekker (2002) and Lathrop (1992) proved that TSS is strongly correlated with band ratios in surface waters that are not much polluted (Nas *et al.,* 2010; Ritchie *et al.,* 1987; Zhou *et al.,* 2006) TP and *chlorophyll-a* were both correlated with band ratio B3/4. Table 12 lists regression equation, R^2 and Sig* values.

Table 4.10. Regression equation, R^2 and Significance values (Sig*) for band ratios

Regression equation	**B1/2**	**B1/3**	**B1/4**	**B2/3**	**B2/4**	**B3/4**
$TSS = y+a*B_i$	0.059(0.4)	0.086(0.4)	0.49(0.29)	0.08(0.39)	**0.64(0.009)**	0.56(0.27)
$TP = y+a*B_j$	0.015(0.5)	0.05(0.3)	0.015(0.6)	0.14(0.8)	0.33(0.11)	**0.38(0.007)**
$Chl\text{-}a=y+a*B_k$	0.00(0.8)	0.00(0.12)	0.35(0.7)	0.41(0.3)	0.63(0.5)	**0.68(0.005)**

Where y and a are regression constant and regression coefficient, B_i, B_j, B_k are band ratios for different WQPs. Thus, our regression model equations for September conditions get these forms:

Table 4.11. Regression equation, R and Sg* values for the chosen model

Regression equation	R	Sig*
TSS = 10.261*B2/4+1.8562	0.95	**0.009**
TP = -10.308*B3/4+2.7101	0.95	**0.007**
Chl-a = -0.2101*B3/4+0.0385	0.97	**0.005**

4.4.4 Statistical results and TSS mapping for September conditions

Total suspended solids are determinant factor in evaluating water clarity. Figure 4.11 shows statistical results for TSS model.

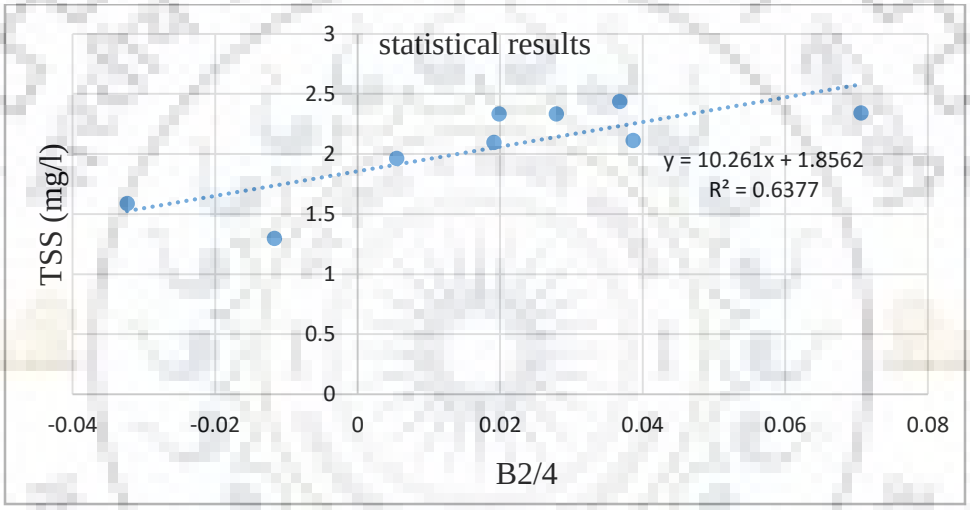

Figure 4.11. Statistical result for TSS chosen model

Figure 4.11 displays TSS regression model. The predicting power of the model, R^2 is 0.64 and significance value, sg* is 0.009 (< 0.05 P-value). Figure 4.12 compares predicted vs actual TSS values. Actual values were little bit high compared to predicted one for September conditions and the level of correlation between actual and predicted values was 0.95. Using ArcGIS software, the TSS spatial distribution was generated (figure 4.13). The map successfully shows the spatial pattern of TSS in lake Tumba. TSS concentrations found in this lake varied between 1.5 and 3 mgl^{-1} during observed September conditions. High TSS concentrations were recorded at village Ikoko (2.761mg/l), inflow bikoro (2.4mg/l) and near village tondo (2.3 mg/l), and could be due to sedimentation from deforestation, land degradation due to forest management practices (logging) as well as slash from burning agriculture.

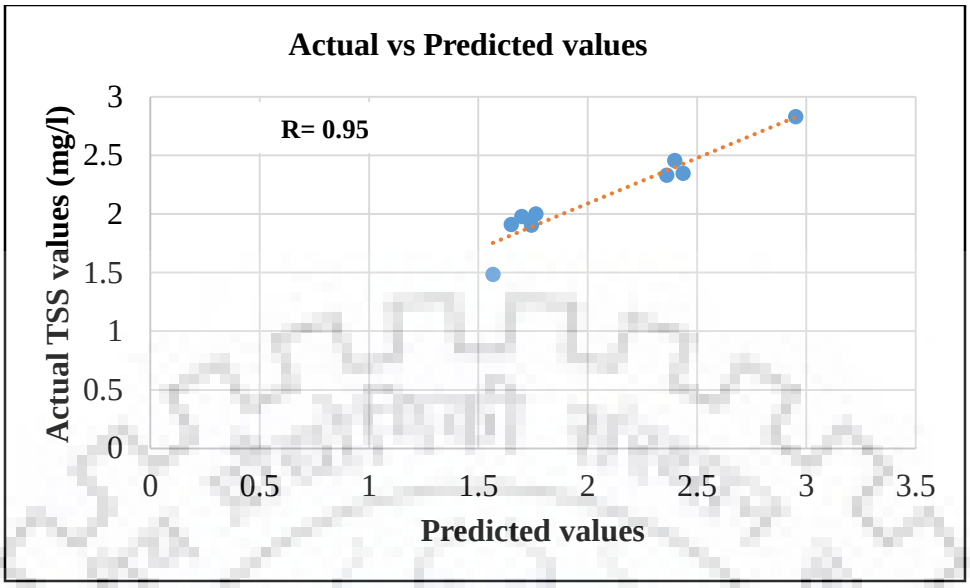

Figure 4.12. Comparison between actual and predicted TSS values

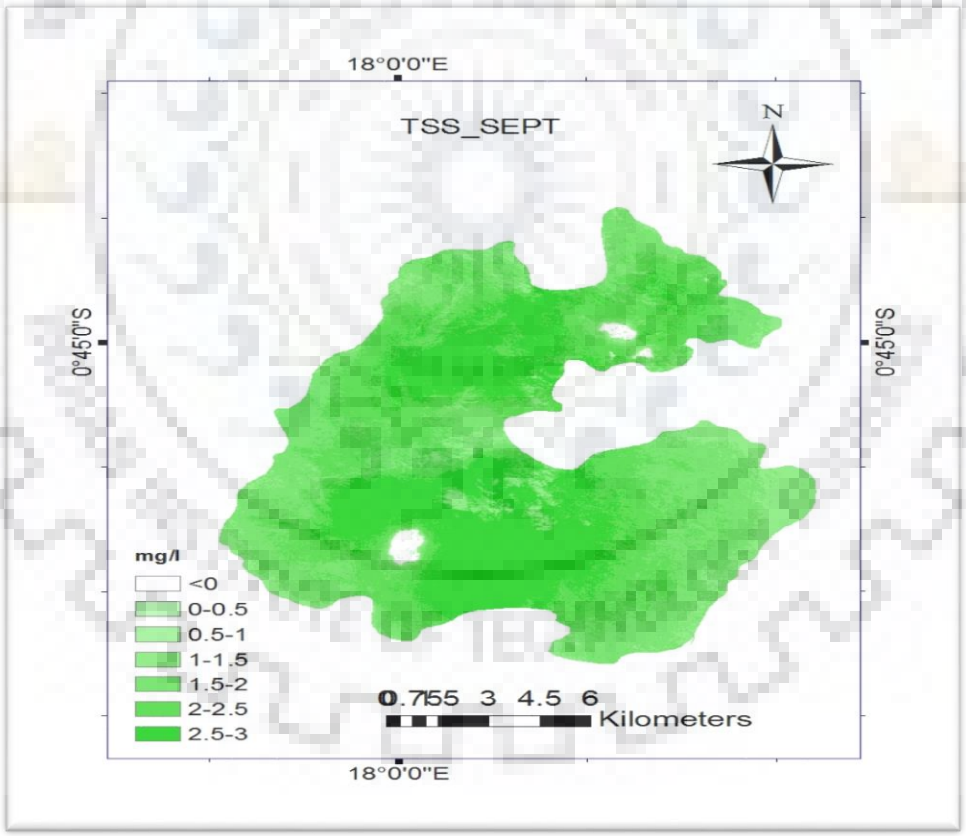

Figure 4.13.Spatial TSS variation in lake Tumba

4.4.5 Statistical results and TP Mapping

Total phosphorus plays an important role in evaluating eutrophication in surface waters. Figure 4.14 shows TP regression analysis results.

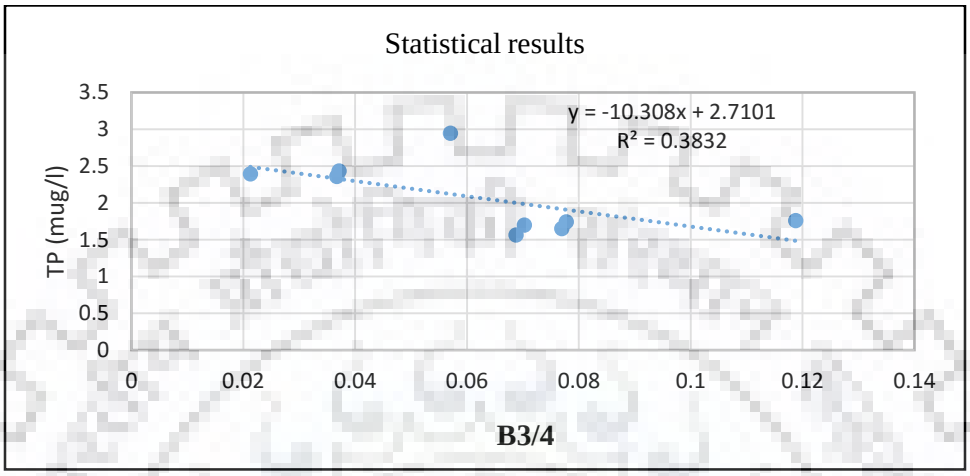

Figure 4.14. Statistical results for TP chosen model

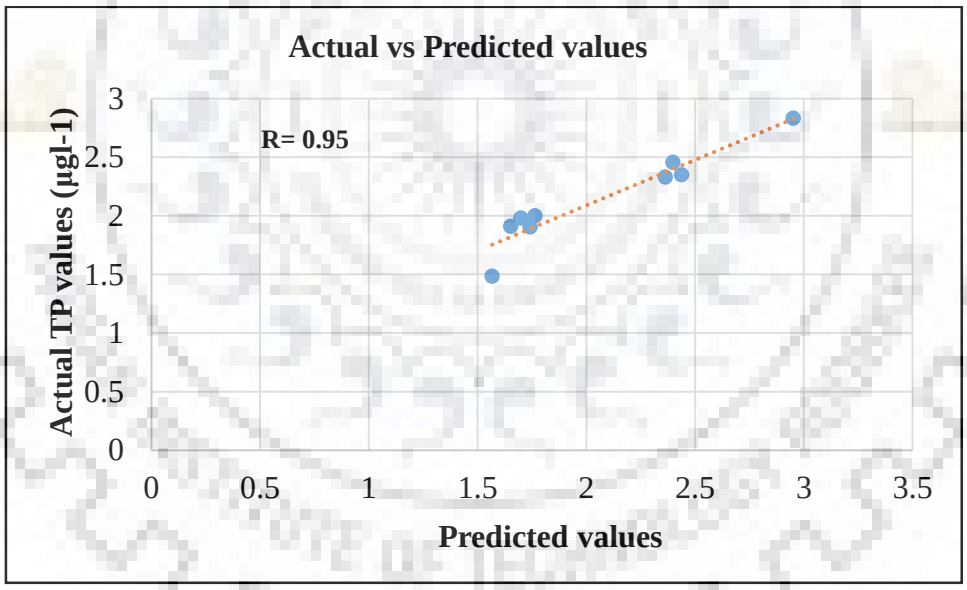

Figure 4.15 Comparison between actual and predicted TP values

Figure 4.14 shows TP regression model. The predicting power of the model, R^2 is 0.38 and significance value, sg* is 0.007 (< 0.05 P-value). Figure 4.15 compares predicted vs actual TP values. Actual values were little bit less compared to predicted one for September conditions with a correlation level R = 0.95. Using ArcGIS software, the TP spatial distribution was generated (figure 4.16). The map successfully shows the spatial pattern of TP in lake Tumba. During

September conditions Total phosphorus in lake Tumba ranged from 1.6 to 3 μgl^{-1} High TP levels were found near lake surface5, inflow lokongoli, village lokongoli, and could be due to waste disposal from surrounding villages but also from plant poison used by men-fishers.

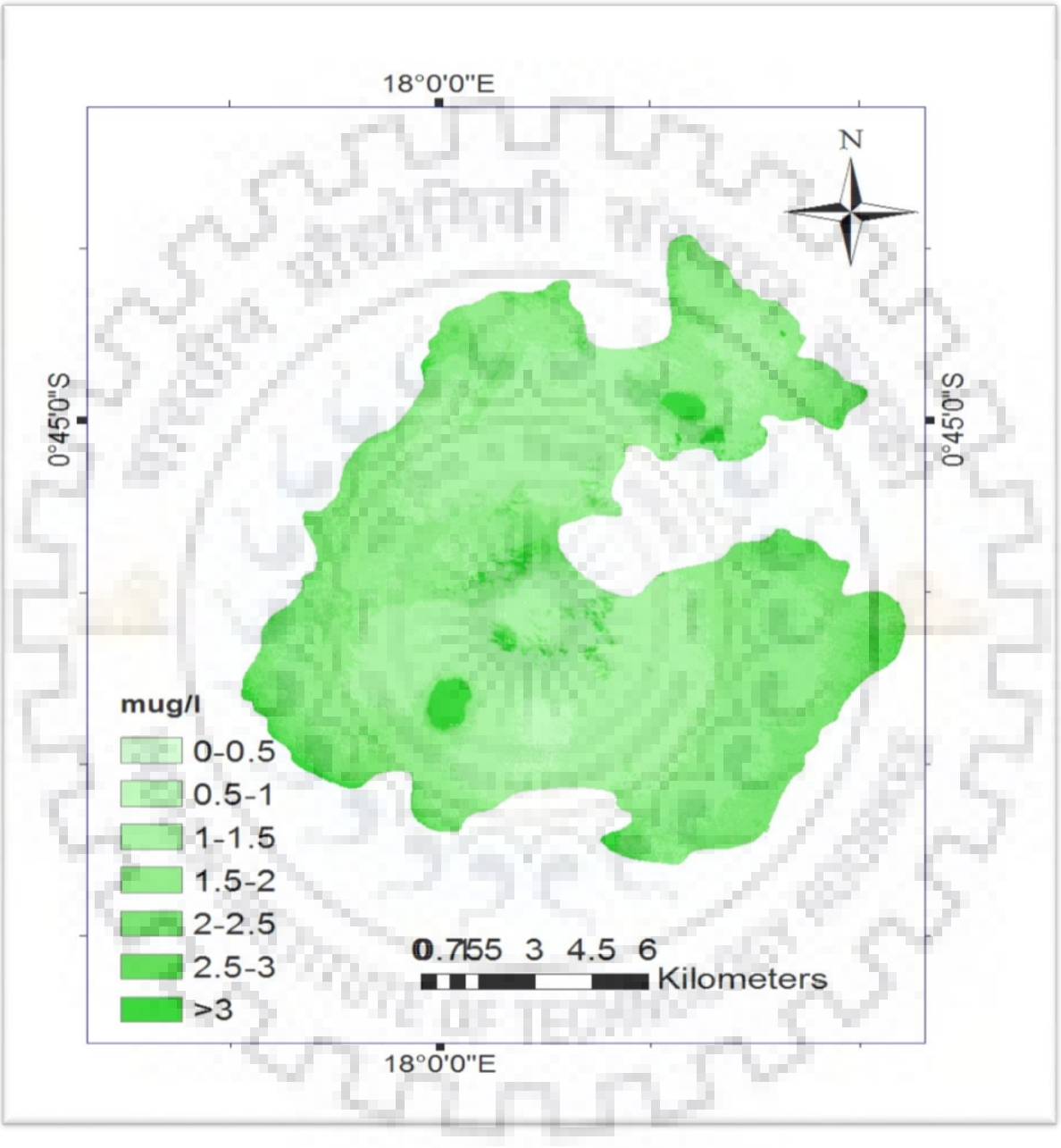

Figure 4.16. Spatial TP variation in lake Tumba

4.4.6 Statistical results and *Chl-a* mapping

Chlorophyll-a is commonly used as an indicator of water quality. It is a pigment found in all plants that is very useful for photosynthesis process. Figure 4.17 shows *Chl-a* regression model results.

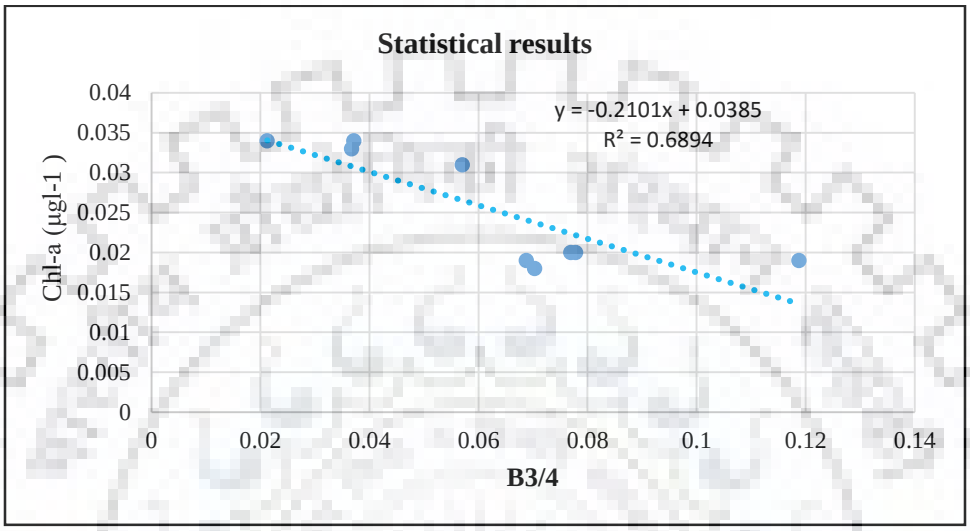

Figure 4.17. Statistical results for Chl-a chosen model

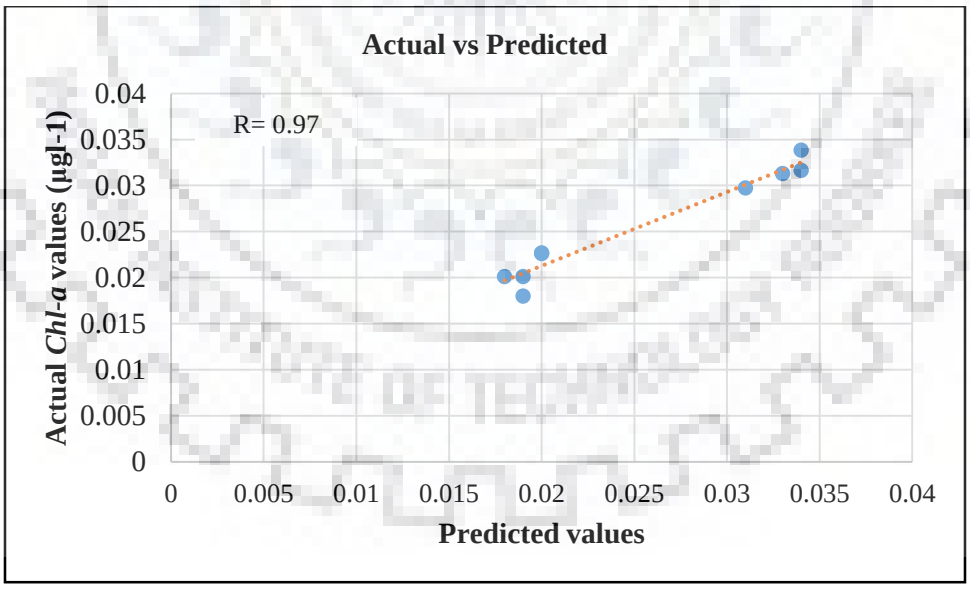

Figure 4.18. Comparison between actual and predicted Chl-a values

Figure 4.18 shows Chl-a regression model. The predicting power of the model, R^2 is 0.68 and significance value, sg* is 0.005 (< 0.05 P-value). Figure 4.19 compares predicted vs actual *Chl-a*

values. Actual values were for the most of sampling points little bit high compared to predicted one. Using ArcGIS software, the *Chl-a* spatial distribution was generated (figure 4.19). The map successfully shows the spatial pattern of ***Chl-a*** in lake Tumba. ***Chl-a*** in lake Tumba ranged from 0.018 to 0.038 μgl^{-1}. The high concentrations_were found near lake surface2, village lokongoli, village nkoso, and could be due to waste disposal from surrounding villages.

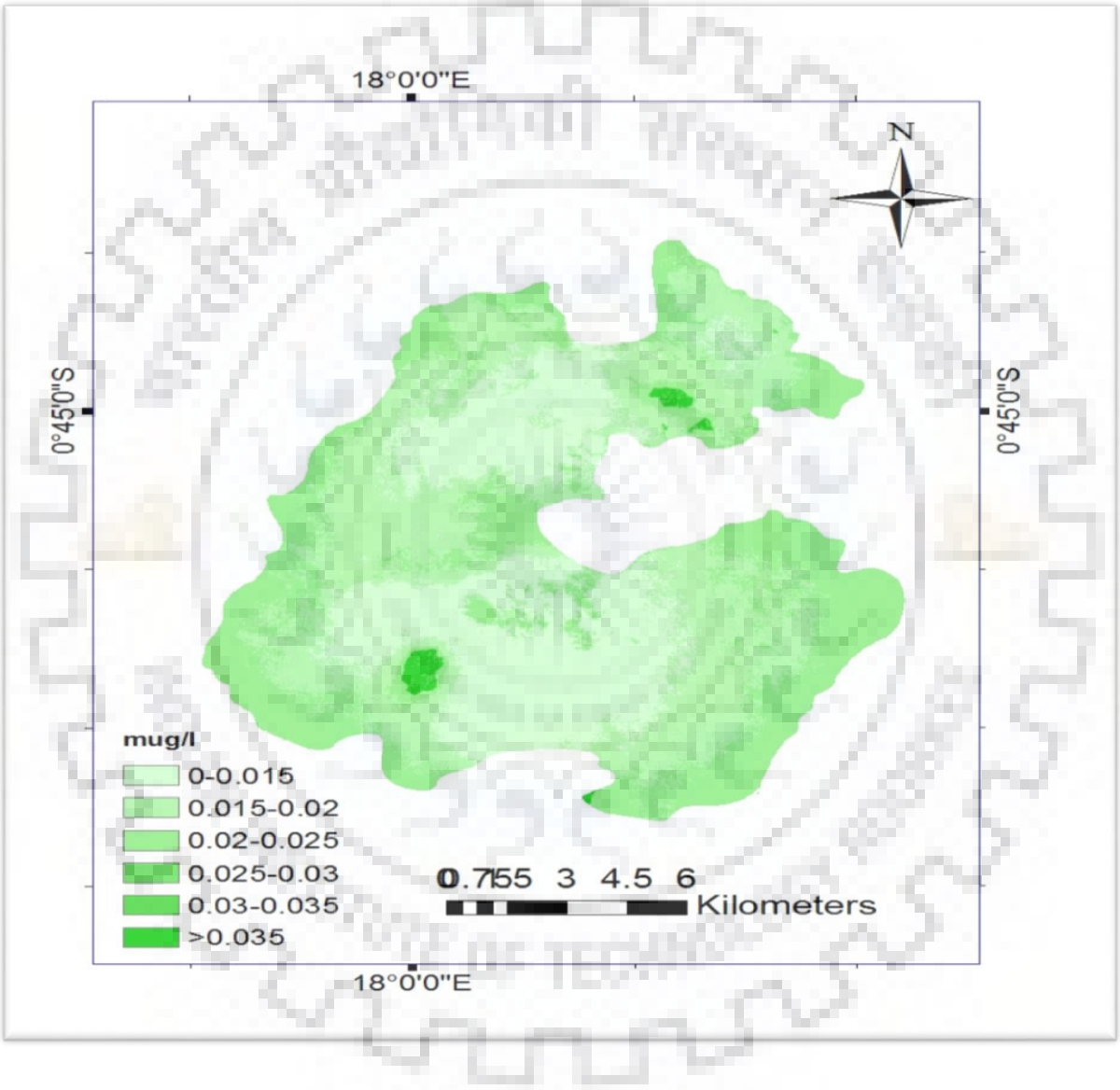

Figure 4.19. Spatial Chl-a variation in lake Tumba

4.5 Remote sensing aided water quality assessment for October 2018

4.5.1 Monitored water quality variables

Table 4.12. October TSS, TP, *Chlorophyll-a* and Tb values

Sample	TSS (mg/l)	TP (μgl^{-1})	Chl-a (μgl^{-1})	Tb (NTU)
1	1.587	2.398	0.034	11.126
2	2.112	2.111	0.036	10.121
3	2.301	2.371	0.039	12.987
4	1.765	2.318	0.038	9.985
5	1.821	2.998	0.034	11.432
6	1.221	2.837	0.035	11.876
7	1.962	2.362	0.033	8.983
8	2.103	3.054	0.029	9.659
9	2.096	2.951	0.031	10.511
10	1.296	2.437	0.034	10.651
11	2.761	3.453	0.025	9.111
12	2.436	1.651	0.02	8.866
13	2.334	1.567	0.019	7.254
14	2.341	1.763	0.019	7.312
15	2.111	1.742	0.02	7.121
16	2.332	1.699	0.018	7.324
17	2.342	1.691	0.018	7.431
18	2.311	1.571	0.018	7.323

Table 4.12 shows the laboratory concentrations of TSS, TP, *Chlorophyll-a* and Turbidity found at the eighteen sampling points. Turbidity failed to show reasonably good correlation for linear bivariate regression model. Only three parameters (TSS, TP, *Chl-a*) were considered in this particular study, for both September and October dataset. The highest amount of TSS (2.761mg/l) was recorded near the Inflow village Ikoko. The highest amount of TP was recorded at lake surface5, inflow lokongoli. *Chlorophyll-a* levels were relatively low for this time of sampling because vegetation has not bloomed full and conditions are not favorable for algae growth.

4.5.2 Correlating water quality variables and reflectance

The table 4.13 lists band mean reflectance values for all 18 sampling points. The table 4.14 shows the Pearson correlation coefficients (R and Sg*) of October monitored variables (TSS, TP and *Chl-a*). Different correlation values were recorded for each band/band ratios and each water quality variable.

Table 4.13. Mean band reflectance for each sampling points

Sample	Band 1	Band 2	Band 3	Band 4
1	0.033718	0.026458	0.030182	0.032982
2	0.034314	0.026573	0.030439	0.034219
3	0.027911	0.019637	0.023037	0.020317
4	0.030985	0.022822	0.025555	0.025149
5	0.046125	0.039517	0.04243	0.058481
6	0.047141	0.040717	0.043894	0.059506
7	0.050776	0.043675	0.047724	0.056514
8	0.032613	0.023975	0.026699	0.026632
9	0.029402	0.021824	0.024968	0.025804
10	0.030634	0.023232	0.026596	0.028803
11	0.040676	0.032884	0.035273	0.052994
12	0.041429	0.033695	0.037624	0.042111
13	0.04686	0.040377	0.044424	0.050252
14	0.040618	0.032058	0.036813	0.032061
15	0.034395	0.026713	0.031311	0.02444
16	0.033361	0.025652	0.03027	0.022453
17	0.030851	0.022687	0.027266	0.020414
18	0.035654	0.027324	0.0318	0.030242

Neither single band nor band ratios have showed good correlation with TSS and Chl-a for October image. This could be due to the impact of the cirrus clouds band (9^{th} band). Only TP has strongly correlated with band ratio (B3/4) as in previous case (September image).

4.5.3 Pearson correlation matrix

Table shows correlation coefficients between water quality variables, bands and band ratios for October conditions.

Table 4.14: Pearson correlation coefficients between water quality parameters and Landsat8 bands and band ratios

	Band1	Band2	Band3	Band4	B1/2	B1/3	B1/4	B2/3	B2/4	B3/4	BNDVI	GNDVI	NDVI
TS r	-0.04	-0.08	-0.05	-0.15	0.15	0.24	0.06	-0.20	0.25	0.24	-0.24	-0.25	-0.24
Sig*	0.87	0.75	0.82	0.52	0.54	0.79	0.32	0.41	0.31	0.31	0.32	0.31	0.31
TP r	-0.05	-0.05	-0.07	-0.06	0.04	-0.41	0.37	0.41	-0.52	**-0.53**	0.41	0.52	0.53
Sig*	0.82	0.81	0.77	0.80	0.87	0.08	0.12	0.08	0.02	**0.02**	0.08	0.02	0.02
Chl r	-0.08	-0.06	-0.13	0.18	0.15	0.02	0.22	0.03	-0.02	-0.02	-0.02	0.02	0.02
Sig*	0.73	0.79	0.58	0.45	0.54	0.91	0.36	0.87	0.92	0.92	0.91	0.92	0.92
Tb r	-0.07	-0.06	-0.04	-0.15	0.13	0.29	-0.03	-0.26	0.32	0.32	-0.29	-0.32	-0.32
Sg*	0.77	0.81	0.87	0.53	0.58	0.22	0.89	0.27	0.18	0.18	0.18	0.18	0.18

4.6 Model validation

The validation was done in two steps:

1. September image data: only the clear part of the lake Tumba was divided in two parts, one containing 5 points and another containing 4 points. The model developed for 4 points showing good correlation was validated against 5 points data. The table below shows the model regression equation and the percentage of correlation between actual and predicted values.

Table 4.15. Regression equation, R^2 of the chosen model and R and Sig* values of actual and predicted values.

Regression equation	**R^2**	**R**	**Sig (<0.05)**
TSS= 14.52*b2/4+1.83	0.70	0.92	0.01
TP= -19.33*b3/4+2.98	0.85	0.97	0.04
Chl-a= -0.345*b3/4+0.04	0.88	0.96	0.02

The figures 4.20 – 4.23 show the comparison between actual and predicted values.

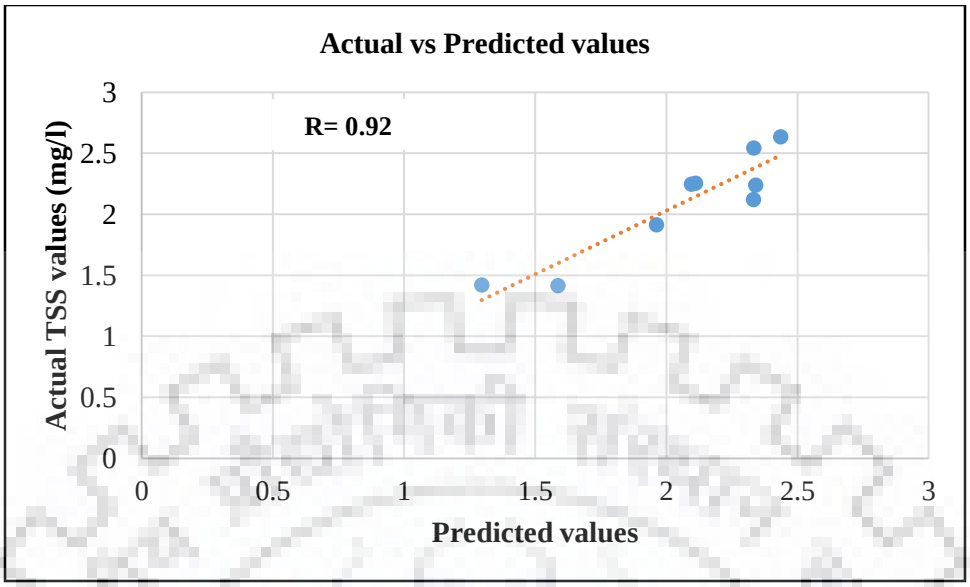

Figure 4.20. Comparison between actual and predicted TSS values

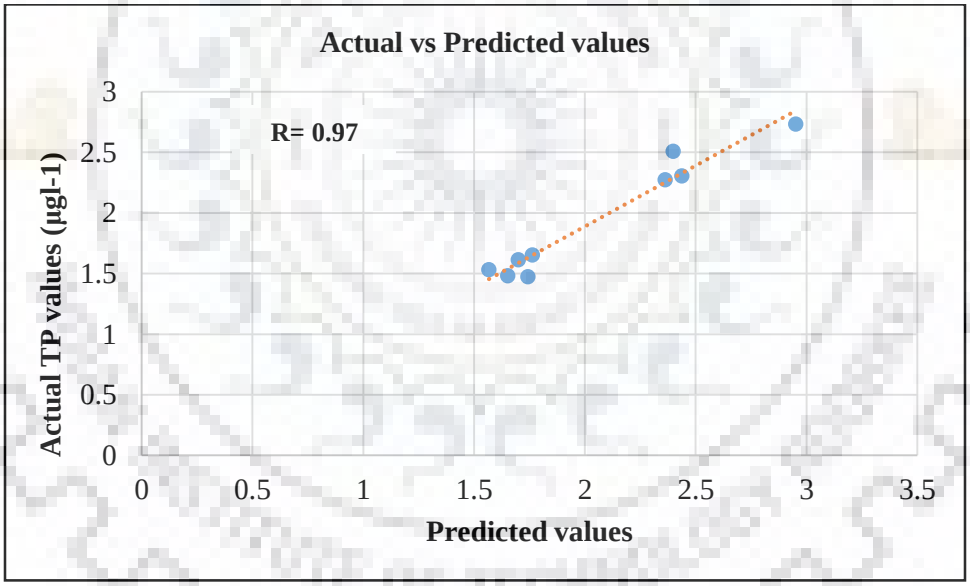

Figure 4.21.Comparison between actual and predicted TP Values

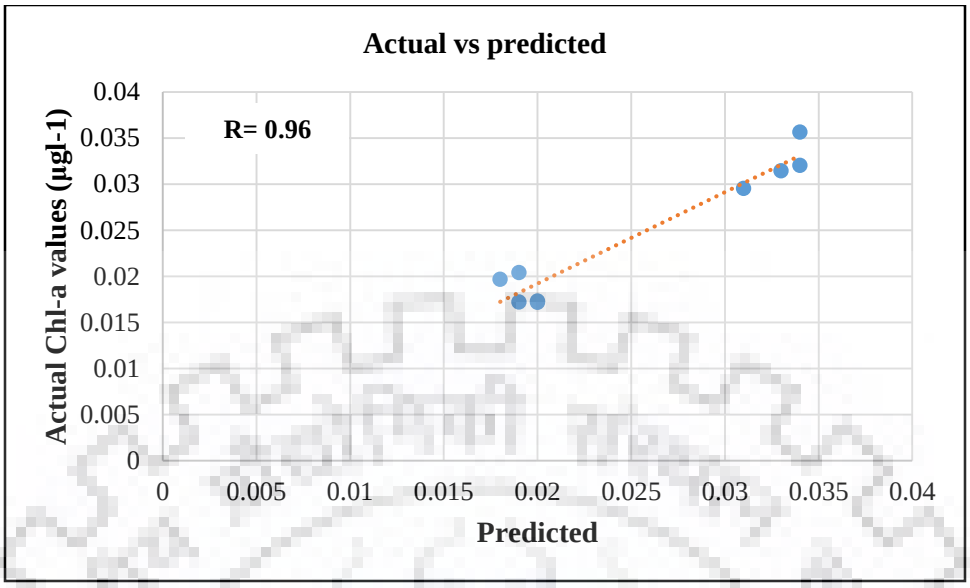

Figure 4.22.Comparison between actual and predicted *Chl-a* values

For October image, we applied the September model (all 9 points of the clear part of the lake Tumba) to check whether the model is good or not. All 18 sampling points for the entire lake were considered. The figures 15 shows comparison between actual and predicted values for September model checked on October image

2. For both September and October images: Employing both September and October images: The model developed employing all 9 points of the clear part of the lake Tumba from the September data was validated against all the 18 point TP data for October image. Actual and Predicted values were correlated to a level of 0.93, means 93 percent. The figure below shows the comparison between actual and predicted values.

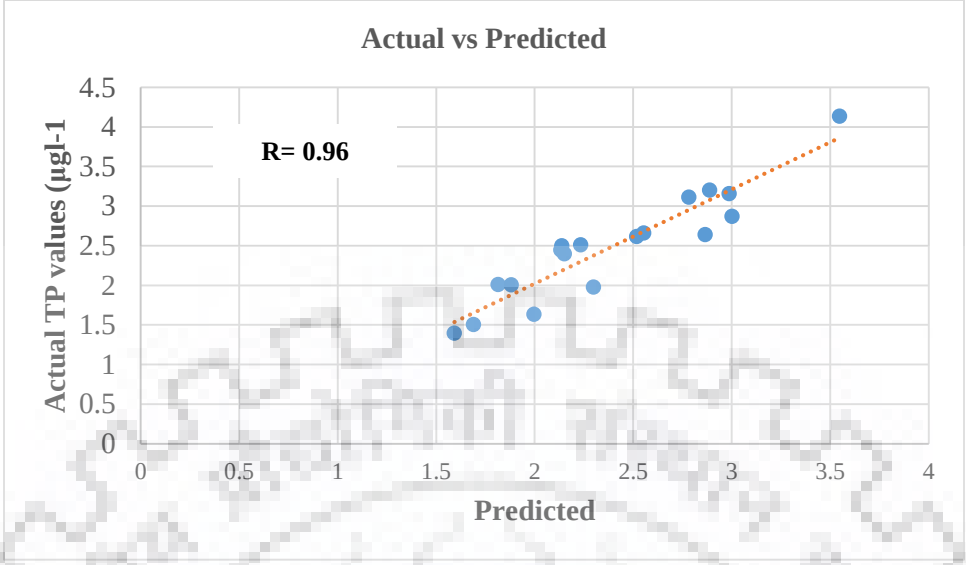

Figure 4.23. Comparison of actual vs. Predicted values.

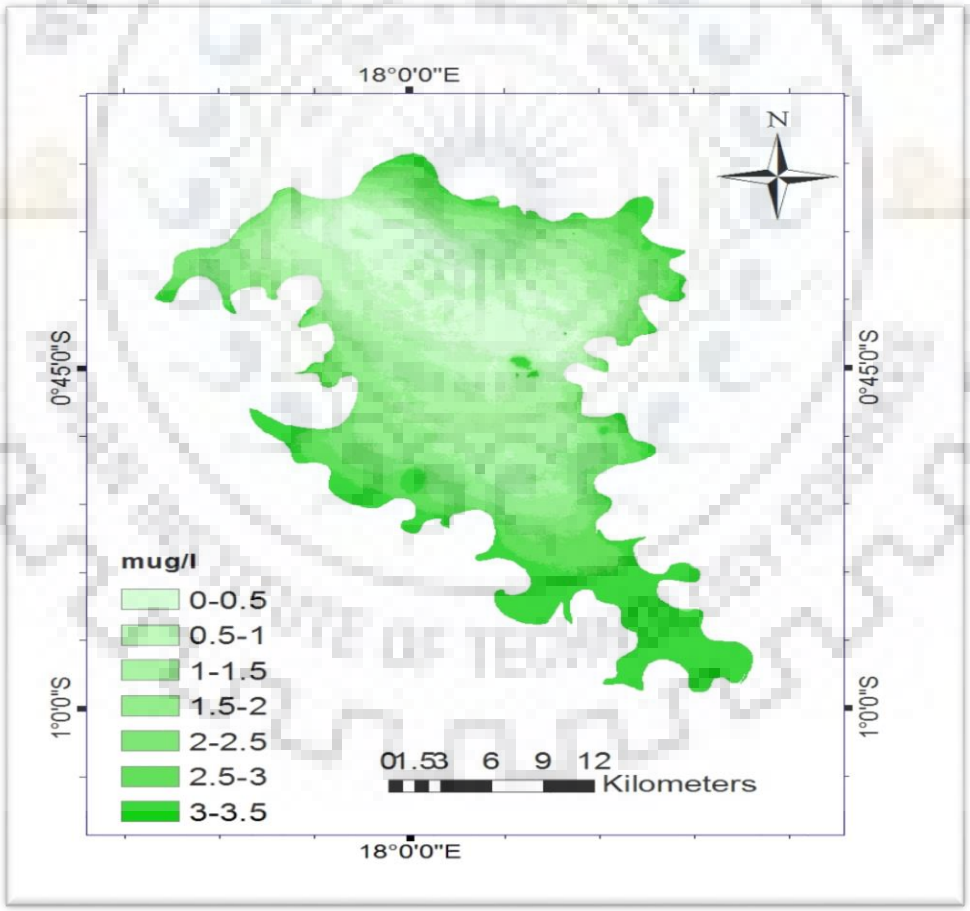

Figure 4.24. Spatial TP variation in lake Tumba for October conditions.

CHAPTER FIVE

FINDINGS AND RECOMMENDATIONS

5.1 Findings

Remote sensing techniques allowed to map and estimate water quality parameters in lake Tumba even during rainy conditions. Turbidity has not given good reasonable results for both September and October conditions. Therefore, only 3 parameters, TSS, TP and Chl-a were considered for the estimation. No single band has showed strong correlation with above water quality parameters under this study. However, band ratio (B2/4) was strongly correlated with TSS for September conditions.

Bivariate regression model (equation 1/Table 4.10) served to predict and map TSS spatial variability in lake Tumba. TP and *Chl-a* showed a good correlation with band ratio (b3/4) for September conditions. Regression models (equation 2 and 3/Table 4.10) could predict and map the spatial variability of TP and *Chl-a* in lake Tumba for September conditions. Out of the data of 9 points considered for remote sensing assessment, model developed from 4 points was successfully validated against the remaining 5 points.

Higher levels of TSS within this water body was found near village Ikoko, inflow bikoro and village tondo, and could be due to sedimentation from deforestation, land degradation due to forest management practices (logging) as well as slash from burned agriculture. Higher levels of TP and *Ch-a* were found near lake surface5, inflow lokongoli, village lokongoli, village Ikoko, lake surface2, and could be due to waste disposal from surrounding villages. For October conditions, TSS and *Chl-a* did not show good correlation, maybe due to the impact of cloud in ninth band of October image. Hence, only TP values could be modelled and a map was produced. Also, model developed employing all the 9 points of September data could be successfully validated against the October data. During October conditions, the water quality parameters were slightly high compared to September conditions.

No study of this kind has been done before for this lake due to the lack of understanding about the subject as well as of subsequent resources for lake monitoring. For the first time, regressions models were developed as a part of this research. The encouraging results of the validation of models in this study demonstrated that remote sensing combined with monitored

water quality can predict TSS, TP and *Chl-a* even for rainy conditions for synoptic lake Tumba water quality.

5.2 Recommendations

Lot of limitations or challenges were faced during the period of this research. The most important were: lack of free cloud images, lack of relevant information about climatic data of the lake Tumba catchment, and also the lack of subsequent resources for more detailed analyses of other important water quality variables. Following the above, we recommend:

- Conduct the entire exercise for the dry season conditions and compare the results.
- Develop a good water quality monitoring network, analysis infrastructure and process protocol for the lake Tumba.
- Develop a Hydro-meteorological monitoring infrastructure for the lake catchment.
- Considering the importance of this lake, plan and initiate more scientific studies on this lake and its catchment on various aspects e.g. Hydrological, Limnological, Socio-economic etc. to arrive at and develop sound management policies.

REFERENCES

Alphan, H. (2003). Land use change and urbanization in Adana. *Turkey. Land Degradation and Development*, 575–586.

APHA. (1992). *Standard Methods of Water and Wastewater.* Washington D.C.: American Public Health Association, American Water Works Association, Water Environment Federation publication.,18th edetion.

Arar, E. J., & Collins, G. B. (1997). *Method 445.0 In vitro determination of chlorophyll-a and pheophytin-a in marine and freshwater algae by fluorescence.* U.S. Enviro: National Exposure Research Laboratory, Office of Research and Development, revision 1.2.

Brivio, P. A., Giardino , C., & Zilioli , E. (2001). Validation of satellite data for quality assurance in lake monitoring applications. *Sci Total Environ*, 3–18.

Chapman, D. (1996). *Water Quality Assessments: A Guide to use Biota, Sediments and Water in Environmental Monitoring* (2nd ed.). E&FN Spon UNESCO/UNEP/WHO,USA.

Chavez, P. J. (1996). Image-based atmospheric corrections- revisited and improved. Photogrammetric Engineering and Remote Sensing. 1025-1036.

Coppin, P., Jonckheere, I., Nackaerts, K., & Muys, B. (2004). Digital change detection methods in ecosystem monitoring: a review. International Journal of Remote Sensing. 1565–1596.

Dekker, A. G., & Peters, S. W. (1993). The use of the Thematic Mapper for the analysis of eutrophic lakes: A case study in the Netherlands. International Journal of Remote Sensing. 799-822.

Dinerstein, E., Kamdem Toham, A., Burgess, N., & Olson, D. (2005). *Freshwater ecoregions of Africa andMadagascar: a conservation assessment.* Washington DC, USA.: Island Press.

Emmerth, P. P., & Bayne, D. R. (1996). Urban influence on phosphorus and sediment loading of West Point Lake, Georgia. Water Resources Bulletin. 145-154.

EPA. (1994). *What is nonpoint source (NPS) pollution? EPA-841-F-94-005. U.S. Environmental Protection Agency*. Retrieved from http://www.epa.gov/owow/nps/qu.html.

EPA. (2012). *EPA.. 5.5 Turbidity. In Water: Monitoring & Assessment. Retrieved from*. Retrieved from Water.epa.gov: http://water.epa.gov/type/rsl/monitoring/vms55.cfm.

ERDAS , F. (1999). *Earth Resources Data Analysis System.* Atlanta, Georgia,: ERDAS Inc.

FAO. (2012). *Information on fisheries management in the Democratic Republic of Congo.* Kinshasa DR Congo: FAO.

Fayma, M. M., & Ghosh , N. L. (2017). Remote estimation of water quality parameters of Himalayan Lake (Kashmir) using Landsat 8 OLI Imagery. *Geocarto International*, 274-285.

Forrer, D. C. (2012). *Applications of Landsat -5 TM Imagery in assessing and mapping water quality in Bankhead Reservoir of the black warior River. A thesis.* TUSCALOOSA, ALABAMA: Department of Geography of the university of Albama.

Hambrook , B., & Conova, M. G. (2007). *Chapter 7.4, Algai biomass indicators:*. U.S. Geological Survey Techniques of Water-Resources Investigations, book 9, chap 7.4, https://doi.org/10.3133/twri09A7.4.

Han, L. (1997). Spectral reflectance with varying suspended sediment concentrations in pure and algal-laden waters. Photogrammetric Engineering and Remote Sensing. 701- 705.

Hughes, R. H., & Hughes, J. S. (1992). *A directory of African wetlands.* Gland, Switzerland, Nairobi, Kenya, and Cambridge, UK: IUCN, UNEP, and WCMC.

Jensen, J. (1996.). Introductory Digital Image Processing: A Remote Sensing Perspective, second ed. Prentice Hall. 316.

Jisang Lim, & Mihla Choi. (2015). Assessment of water quality based on Landsat 8 operational land imager associated with human activities in Korea. *Environ Monit Assess*, 384.

Kamdem, A., Amico.J. Olson, D., Blom, A., Trowbridge, L., Bourgess, N., Thieme, M., . . . Strand, H. (2006). *A vision for biodiversity conservation in central Africa: Biological priorities for conservation in the Guinean-Congolian forest and freshwater region.* Washington, DC 20037-1193 USA: World Wildlife Fund (WWF).

Kashaigili, J. (2006). Landcover Dynamics and Hydrological Functioning of Wetlands in the Usangu Plains in Tanzania PhD Thesis, Sokoine University of Agriculture. 266.

Kashaigili, J. J., Mbilinyi, B. P., & Mccartney, M. M. (2006). Dyanamics of Usangu plains wetlands: use of remote sensing and GIS as management decision tools. Physics and Chemistry of the Earth. 969–975.

Khattab MFO, & Meerkel BJ. (2013). Application of Landsat 5 and Landsat 7 images data for water quality studies in New York Habor. *Estuarine Coastal Shelf Sci*, 437-448.

Koltas, V. e. (2012). *Water quality monitoring and assessment,* (1st Ed ed.). CROATIA: p. cm. ISBN.

Koltas, V., & Dimitra, V. (2012). *Water Quality Monitoring and Assessment.* Rijeka, Croatia: Janeza Trdine.

Kondratyev KYA, Pozdnyakov DV, & Patterson LH. (1998). Water quality remote sensing in the visible spectrum. *Int J Remote sens*, 957-979.

Kumar, D. (2018). *Fundamentals of Water Pollution.* Delhi, India:: Vinod Kumar Jain Scientific International.

Lathrop, R. (1992). Landsat Thematic Mapper monitoring of turbid inland water quality. *Photogrammatric Engineering and Remote Sensing*, 465–470.

Lévêque, C. (1997). *Biodiversity dynamics and conservation: The freshwater fish of tropical Africa*. Cambridge, UK: Cambridge University Press.

Matthes, H. (1998). Lake Tumba's fish and Ikela region: Systematic and Ecological study. . *Animals of the Royal Meseum of Central Africa*, 126-204.

Mputu, A. (2013). *Aquatic Assessment in the Lake Tumba Landscape, DRCongo: Fish Diversity and Conservation. Licentiate Thesis.* Uppsala: Department of Aquatic Sciences and Assessment.

Mundia, C. N., & Aniya M, M. (2006). Dynamics of land use/cover changes and degradation of Nairobi city, Kenya. Land Degradation and Development. 97–108.

Murphy, B., Clay H, & Wadzuk. (2009). Hydraulic evolution and Total Suspended Solids capture of an infiltration trench. *Wiley interSccience*, 108-114.

Mushtaq , F., & Pandey , A. (2014). Assessment of land use/land cover dynamics vis-à-vis hydro meteorological variability in Wular Lake environs Kashmir Valley, India using multitemporal satellite data. *Arab J Geoscie*, 4707–4715.

Nas, B., Ekercin, S., Karabork, H., & Berktay, A. (2010). An application of Landsat-5 TM image data for water quality mapping in Lake Beysehir, Turkey. Water Air Soil Pollution. 183-197.

Perlman, H. (2014). *Turbidity in The USGS Water Science School*. Retrieved from USGS: Retrieved from http://water.usgs.gov/edu/turbidity.html

Raschke, R. (1993). *Guidelines for Assessing and Predicting Eutrophication Status of small Southeastern Piedmont Impoundments.* Environmental Services Division, Ecological Support Branch: U.S. Environmental Protection Agency Region IV. Athens, GA.

Richards, J. e. (1999). *Remote sensing digital image analysis Vol. 3.* New York: Springer.

Ritchie, J. C., Zimba, P., & Everitt, J. (2003). Remote sensing techniques to assess water quality. Photogrammetric Engineering and Remote Sensing. 695-704.

Ritchie, J. C., Cooper, C. M., & Yongqing, J. (1987). Using Landsat multispectral scanner data to estimate suspended sediments in Moon Lake, Mississippi. Remote Sensing of the Environment. 65-81.

Romshoo, S., & I, R. (2012). Assessing the impacts of changing land cover and climate on Hokersar wetland in India. *Arab J Geosci*, 143-160.

Ronald, M., & Webster , G. (2018). Near real time water monitoring of Chivero and Manyame Lakes of Zimbabwe. *University of Zimbabwe.*, 378-385.

Sciences, N. A. (1969). *Eutrophication: Causes, Consequences, Correctives. Proceedings of a Symposium.* Washington D.C: National Academy of Sciences.

Seker , D., Goksel , C., Kabdasli , S., Musaoglu , N., & Kaya , S. (2003). Investigation of coastal morphological changes due to river basin characteristics by means of remote sensing and GIS techniques. *Water Sci Technol*, 135–142.

Stiassny, M. H. (2007). *Freshwater and brackish freshwater fish from lower Guinea, west Central Africa.* (Vol. 1). Paris: IRD.

Torbick, N., Hession, S., Hagen, S., Wiang, N., & Becker, B. (2013). Mapping inland lake water quality across the Lower Peninsula of Michigan using Landsat TM imagery. *Int J Remote Sens*, 7607–7624.

Wahl, M. H., McKellar , H., & Williams , T. M. (1997). Patterns of nutrient loading in forested and urbanized coastal streams. *Journal of Experimental Marine Biology and ecology*, 111-131.

Wang, F., Han, L., Kung, T., & Van Arsdale, R. B. (2006). Applications of Landat-5 TM imagery in assessing and mapping water quality in Reel Foot Lake, Tennesse. *International Journal of Remote Sensing*, 5269-5283.

Yeh, A., Gar, A., & Xia, L. (1996.). Urban growth management in Pearl River delta: an integrated remote sensing and GIS approach. *ITC Journal*, 77–78.

Yuan, C., & Elvidge, C. (1998). NALC land cover change detection pilot study: Washington DC area experiments. *Remote Sensing of Environment*, 166 –178.

Yuan, F., Sawaya, K. E., Loeffelholz, B. C., & Bauer, M. E. (2005). Land cover classification and change analysis of the twin cities (Minnesota) Metropolitan Area by multitemporal Landsat remote sensing. *Remote sensing of Environment*, 317-328.

Zanga, N. (2013). *Towards Aquatic Assessment of Lake Tumba, DR Congo. Licentiate Thesis.* Uppsala: Faculty of Natural Resources and Agricultural Sciences Department of Aquatic Sciences and Assessment.

Zhang, Y., & Wang, Y. (2002). Assessment of the Impact of Land-Use Types on the Change of Water Quality in Wenyu River Watershed (Beijing, China). *International Perspectives of Environmental Change*, 275-294.

Zhou, W. W. (2006). Mapping the concentrations of total suspended matter in Lake Taihu, China, using Landsat-5 TM data. *International Journal of Remote Sensing*, 1177-1185.